JACS Au
AN OPEN ACCESS JOURNAL OF THE AMERICAN CHEMICAL SOCIETY

pubs.acs.org/jacsau

Perspective

Challenges and Perspectives of Single-Atom-Based Catalysts for Electrochemical Reactions

Jiazhan Li,[‡] Chang Chen,[‡] Lekai Xu, Yu Zhang, Wei Wei, Erbo Zhao, Yue Wu, and Chen Chen*

Cite This: *JACS Au* 2023, 3, 736−755

Read Online

ACCESS | Metrics & More | Article Recommendations

ABSTRACT: Single-atom catalysts (SACs) are emerging as the most promising catalysts for various electrochemical reactions. The isolated dispersion of metal atoms enables high density of active sites, and the simplified structure makes them ideal model systems to study the structure−performance relationships. However, the activity of SACs is still insufficient, and the stability of SACs is usually inferior but has received little attention, hindering their practical applications in real devices. Moreover, the catalytic mechanism on a single metal site is unclear, leading the development of SACs to rely on trial-and-error experiments. How can one break the current bottleneck of active sites density? How can one further increase the activity/stability of metal sites? In this Perspective, we discuss the underlying reasons for the current challenges and identify precisely controlled synthesis involving designed precursors and innovative heat-treatment techniques as the key for the development of high-performance SACs. In addition, advanced operando characterizations and theoretical simulations are essential for uncovering the true structure and electrocatalytic mechanism of an active site. Finally, future directions that may arise breakthroughs are discussed.

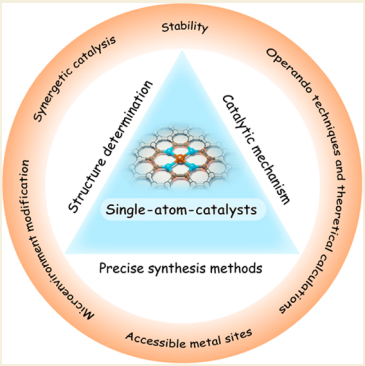

KEYWORDS: *single atom, electrocatalysis, activity, stability, synergetic catalysis*

1. INTRODUCTION

With the global economic growth, the CO_2 emissions and energy demand have increased dramatically. Renewable energy conversion and storage technologies based on electrocatalytic reactions, such as CO_2 reduction reaction (CO_2RR),[1] oxygen reduction reaction (ORR),[2] and water oxidation (hydrogen evolution reaction, HER; oxygen evolution reaction, OER),[3,4] hold great promise to solve the energy and environmental issues. However, the state-of-the-art catalysts for the discussed reactions usually rely on precious metals (platinum,[5] iridium,[6] ruthenium,[7] etc.). The high cost and scarcity of precious metals limit the practical application of electrochemical devices. The development of efficient and cost-effective electrocatalysts is of vital importance and is emerging as a highly prosperous research field.

In recent years, single-atom catalysts (SACs) consisting of a single metal atom as an isolated active site have progressed tremendously and have been identified as the most promising electrocatalysts.[8] Compared with traditional nanoparticle catalysts, the isolated dispersion of metal sites offers a maximized atom utilization, which not only significantly decreases the cost but also leads to excellent catalytic behavior in terms of activity and selectivity.[9] For nonprecious metal catalysts, the elimination of nanoparticles, which are usually low or nonactive for an electrochemical reaction, dramatically increases the density of efficient single metal sites.[10] This breakthrough significantly increases the activity of nonprecious metal catalysts and makes it possible to completely replace precious-metal-based catalysts with nonprecious-metal catalysts. Moreover, the elimination of nanoparticles simplified the components of catalysts, making it an ideal platform on which to perform operando characterizations and theoretical calculations, which could identify the active site structure, uncover the catalytic mechanism, provide fundamental understanding about structure−performance relationships, and finally guide the rational design of high-performance catalysts.[11−13]

In the SACs, the single metal atoms are commonly stabilized by the neighboring atoms in the substrate. The most reported substrates are metal compounds (oxide, hydroxide, sulfide, etc.) and carbon.[14−16] For metal-compound-based SACs, the active-metal single atoms were uniformly dispersed on the surface of the metal compound. Due to the high surface energy, the single atoms are extremely unstable. Thus, the strong interaction between single atoms and support (SMSI), usually through metal bonding between metal and nonmetallic ligands (such as C, N, O, S, and P), is essential for the

Received: January 2, 2023
Revised: January 29, 2023
Accepted: February 1, 2023
Published: February 16, 2023

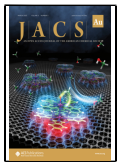

https://doi.org/10.1021/jacsau.3c00001
JACS Au 2023, 3, 736−755

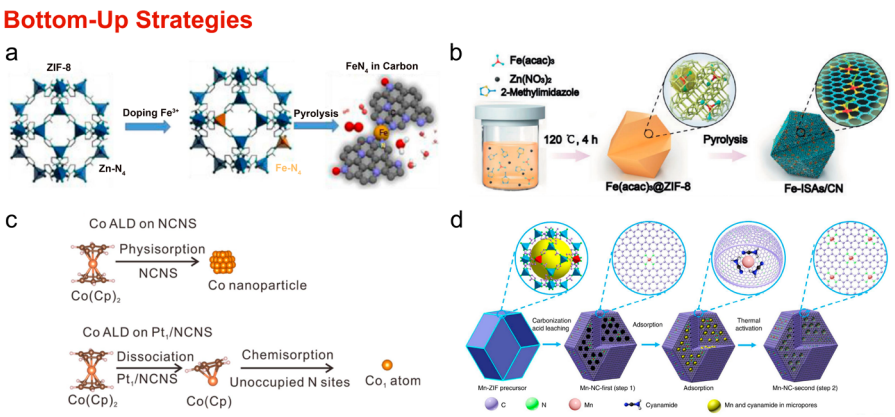

Figure 1. (a) Scheme of synthesis principles of Fe-doped ZIF-derived catalysts. Adapted with permission from ref 40. Copyright 2017 American Chemical Society. (b) Schematic illustration of the formation of Fe-ISAs/CN. Adapted with permission from ref 42. Copyright 2017 Wiley-VCH. (c) Assumption of the Co ALD process on pristine NCNS and Pt_1/NCNS catalysts. Adapted with permission from ref 45. Copyright 2021 Springer Nature. (d) Schematic of atomically dispersed MnN_4 site catalyst synthesis. Adapted with permission from ref 47. Copyright 2018 Springer Nature.

anchoring of the single metal atom. A metal single atom and nonmetallic ligands constitute a metal single-atom site. The nonmetallic ligands not only stabilize the metal single atom but also tune the electronic structure of the metal site, determining the activity, selectivity, and stability of catalysts.[17−20] Carbon materials exhibit good stability, high surface area, excellent electrical conductivity, and flexibility with dopants, which make them a popular substrate for electrocatalysts.[21−23] As the single metal site is usually stabilized by the nitrogen atoms that are doped in the carbon substrate, carbon-based SACs can be labeled as metal−nitrogen−carbon (M−N−C) catalysts.[24−26] The electronic structure of the metal site can be tuned by the number and kind of first-shell or second-shell atoms, such as N, P, S, and O.[27−29] The neighboring metal atom or nanoparticle could also affect the electronic structure of the center metal site.[30−32]

Although the SACs exhibit superior activity for a series of electrochemical reactions, their practical applications in real devices have not been realized. Compared with precious-metal-based catalysts, the activity of SACs is still insufficient. Moreover, the SACs usually suffer rapid activity loss under long-term operating conditions, which is a fatal drawback for a practical catalyst.[33−35] Significant efforts including (1) increasing the density of accessible metal sites, (2) increasing the intrinsic activity of the single metal site, (3) enhancing the stability of SACs, and (4) uncovering the active-site structure and electrocatalytic mechanism should be devoted to promote the practical application of SACs. There have been numerous comprehensive reviews on SACs, especially on the synthesis methods, characterization techniques, and catalytic performances. In this Perspective, we first summarize the current challenges toward further increasing the performance of SACs and then analyze the underlying reasons for the current challenges through discussing the unique properties of SACs. The combination of precisely controlled synthesis, advanced operando characterizations, and theoretical simulations is identified as the key for the development of high-performance SACs. Possible future directions that may arise breakthroughs are also discussed at the end of this Perspective.

2. DENSITY OF ACCESSIBLE METAL SITES

The overall activity of SACs is mainly determined by the number and intrinsic activity of accessible active sites. With a given metal species, the electronic structure and intrinsic activity of the single metal sites obtained by different synthesis methods usually do not show significant differences. For instance, plenty of methods that employ different metal salts and ligands could finally generate similar $Fe−N_4$ structures for ORR.[36] In this view, the main strategy for increasing the activity of SACs is to increase the number of accessible active sites, which could be directly realized by increasing the loading of isolated metal sites. Since the concept of "single-atom catalysts" was formally proposed in 2011,[37] various synthesis methods have been reported to increase the metal loading and great breakthroughs have been achieved. Besides, an appropriate structure of support could also increase the overall activity via increasing the utilization rate of metal sites. In this section, we discuss the challenges and current strategies for increasing the density of accessible metal sites, which are categorized into "increasing the metal loading" and "increasing the utilization of metal sites".

2.1. Increasing the Metal Loading

The way in which single atoms are introduced into the support is a necessary consideration for researchers when designing single-atom catalysts.[38,39] According to the difference of metal precursors, the synthesis strategies of SACs can be categorized into bottom-up strategies and top-down strategies. They undergo different synthetic pathways and face different challenges for increasing the metal loading.

2.1.1. Bottom-Up Strategies. The bottom-up method employs a soluble metal salt or mononuclear metal complex as the metal precursor and usually undergoes a wet-chemistry process to synthesize the precursor or impregnate the metal sites on the support. Besides, heat-treatment is usually necessary for the formation of stable and active metal sites. The key to increase the density of isolated metal sites is suppressing the competitive side reactions that lead to agglomerations.

In the wet-chemistry step, even trace H_2O or O_2 could lead to the hydrolyzation or oxidization of the metal salt. Thus, the trace H_2O in the solvent and even crystal H_2O in raw materials should be seriously considered. Moreover, we could suppress the hydrolysis by constructing a stronger coordination bond between the metal site and organic ligands. Wu and coauthors developed a chemical doping method that directly replaces the Zn nodes with Fe during the growth of zeolitic imidazolate

https://doi.org/10.1021/jacsau.3c00001
JACS Au 2023, 3, 736−755

frameworks (ZIF-8) (Figure 1a).[40] The dissociative Fe^{3+} was captured and stabilized by the nitrogen through the Fe−N coordination bond, which is a strong competitive reaction to the hydrolysis of Fe^{3+} and allows a high concentration of Fe salt. Introducing surfactant or extra ligands to the solution could also prevent the metal ions from undergoing hydrolysis through complexation and thus significantly increase the loading of the metal sites. Xiong and coauthors synthesized Ni/CS single-atom catalysts by adding Ni ions to a solution with dopamine as the carbon template after calcination and etching.[41] The unique hollow structure of a carbon sphere enables a high loading of Ni single atoms. The CO_2RR performance increases with the increase in the number of shells because the higher number of shells represents more active sites exposed. Another strategy to suppress the hydrolysis is to thoroughly escape the dissociation of the metal salt by choosing an appropriate metal precursor, such as acetylacetonate. In this case, the key problem is to realize the uniform and stable load of metal salt on the precursor. Li and coauthors proposed a space confinement strategy to introduce the metal salt to the precursor (Figure 1b).[42] They utilized the unique pore structure of ZIF-8 (pore diameter of 3.4 Å, cavity diameter of 11.6 Å) to separate and encapsulate the $Fe(acac)_3$ (molecular diameter of 9.7 Å), which could maintain the isolated dispersion, and transformed it into $Fe-N_4$ sites during the following heat-treatment process. Currently, spatial confinement has become one of the most common and effective strategies to improve the density of the single atoms, including design of defect sites, interlayer, nanoframework, etc. Deng and coauthors designed a high density of in-plane active sites by confining a large number of Mo single atoms (16 wt %) in the basal-plane lattice of the CoOOH structure.[43] To avoid the stack of two-dimensional MOOH layers, they used ZIF-67 templates to get three-dimensional (3D) cubic hollow nanoframes. The strong interaction between the single atoms and the support can also be used to increase the metal loading. Gu and coauthors reported a high-density single-atom Ir (18 wt %) catalyst on a NiO matrix by using the approach of heating the solution on carbon cloth.[44] Ir atoms are atomically dispersed at the outermost surface of the NiO matrix and are stabilized by covalent Ir−O bonding, which enables a high density of anchor sites and, in turn, Ir atoms. The Ir single atom not only can be used as the active site for OER but also can activate the surface reactivity of NiO, thus significantly improving the OER performance. Atomic layer deposition (ALD) is feasible to obtain different metal single atoms on different matrixes, but the high dissociation barrier and predominantly physical adsorption of metal precursors always lead to low metal loading, especially among carbon-based supports. To solve this issue, Sun and coauthors used the prelocated isolated Pt single atoms as the catalyst to facilitate the dissociation of ALD precursors, thus achieving a high-density Co single atom (Figure 1c).[45] This approach can be easily extended to the synthesis of Fe and Ni single-atom catalysts. Different from laboratory tests, industrial-grade reaction conditions are relatively harsh, often requiring a high density of active sites. A simple and rapid synthesis method is often more conducive to improving the repeatability and scale-up preparation capacity of the catalyst. Zeng and coauthors reported high-density Pt (24 atoms nm^{-2}) and Ir (32 atoms nm^{-2}) single atoms anchored on the $Co(OH)_2$ support for overall water splitting at industrial current densities.[46] They used the electrochemical reduction method to carry out a one-step coreduction of the metal precursors to obtain a high-loading SAC. This one-step approach can also be used to synthesize 20 other kinds of SACs.

In the thermal activation/carbonization step, the high temperature could endow energy to the single atoms and stimulate their mobility. If the metal−support interaction is not strong enough to resist the mobility, and if the thermal stability of the support-anchored metal sites is inferior to that of the metal clusters, the single atoms would migrate and spontaneously transform into metal clusters. A high metal loading usually means a short distance between two metal sites, which makes agglomeration of the metal sites easier. Thus, a higher metal loading usually calls for stronger metal−support interaction. Moreover, the thermal stability of the support should also be considered, as the heat-treatment may lead to metal agglomeration by changing or ruining the structure of the support. For the carbon-based SACs, carbon atoms at high temperature could inevitably serve as a reductant to break the bond between the metal sites and the substrate, and the high temperature could also lead to the dissociation and volatilization of nitrogen atoms, which are the main anchor sites of the isolated metal atoms. In this regard, preventing the nitrogen loss and minimizing the time of heat-treatment would be effective. Besides, introducing a nitrogen-rich sacrificial agent to the system could increase the nitrogen anchor sites on the support and thus the isolated metal sites. Wu and coauthors reported a two-step chemical doping−adsorption method to increase the metal loading step-by-step; the first step obtained a Mn and N codoped carbon support with abundant micropores, which were employed as the host to adsorb Mn ions and an additional nitrogen source in the adsorption step (Figure 1d).[47] The addition of a nitrogen source, such as cyanamide, phenanthroline, dipicolylamine, and melamine, could not only promote the micropore adsorption of Mn but also provide a benefit for the maintenance of isolated Mn by providing N anchor sites. Besides directly adding nitrogen sources to the precursor, we can also put the nitrogen source upstream of the furnace.[48] The separation of nitrogen source and support allows a lower decomposition temperature for the nitrogen source and makes it possible to continuously provide N to the support.

2.1.2. Top-Down Strategies. The top-down strategies employ bulk or nanostructured metal as the metal precursor, which would transform into stable single atoms on the support at specific conditions. The key steps for the top-down method are detaching the surface atoms from the bulk metal and capturing the detached metal atoms with an appropriate support. According to the driven force of metal detachment, the top-down methods can be subdivided into thermochemical and electrochemical. For a long time, chemical vapor deposition (CVD) technology has been routinely applied to the growth of various thin-film materials on various substrates. CVD is a process in which volatile precursors react in the gas phase or on the substrate surface and finally form low-dimensional products deposited on the substrate. As far as the whole conversion process and products are concerned, these CVD-assisted strategies can be applied to the synthesis of SAC catalysts. A carbon support with fine structure is designed in advance, and then metal single atoms are prepared by the CVD method. The CVD method could not only provide sufficient metal sites to the support but also benefit the utilization of active sites, as the obtained metal sites usually locate at the surface of the support. For the CVD method, detaching the

https://doi.org/10.1021/jacsau.3c00001
JACS Au 2023, 3, 736−755

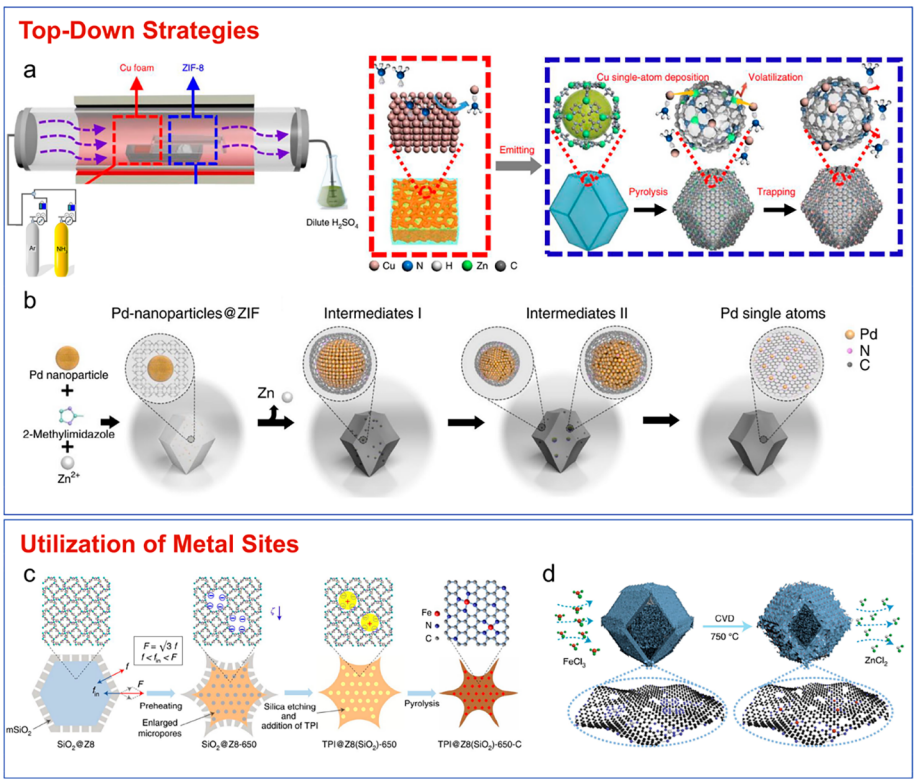

Figure 2. (a) Schematic of the preparation of Cu-SAs/N−C. Adapted with permission from ref 49. Copyright 2018 Springer Nature. (b) Scheme of the transformation of nanoparticles to single atoms. Adapted with permission from ref 50. Copyright 2018 Springer Nature. (c) Schematic synthesis process of TPI@Z8(SiO_2)-650-C by silica coating, preheating, etching silica off, absorbing TPI, and carbonization. Adapted with permission from ref 54. Copyright 2019 Springer Nature. (d) Scheme of synthesis of FeNC-CVD-750 via $FeCl_3$ CVD. Adapted with permission from ref 55. Copyright 2021 Springer Nature.

surface atoms from the bulk metal is a key step. Li and coauthors employed ammonia gas as an assistant to detach and transport the metal atoms at high temperature (Figure 2a). Through the strong Lewis acid−base interaction, the ammonia could coordinate with copper atoms to form volatile $Cu(NH_3)_x$ species, which could flow under the ammonia atmosphere and finally be trapped by the defects on the nitrogen-rich carbon support, forming the isolated copper sites.[49] Without the assistance of ammonia gas, we could also realize the top-down transformation by directly arranging the bulk metal adjacent to the defect of the support. Li and coauthors encapsulated the Pd nanoparticles in the ZIF-8 precursor and then performed a high-temperature treatment (Figure 2b).[50] They proved that the Pd nanoparticles could transform into thermally stable Pd−N_4 single-atom sites when the temperature is >900 °C. Wu and coauthors observed that nano-FeO_x particles encapsulated in the nitrogen-doped carbon could transform into thermally stable Fe−N_4 sites when the when the temperature is >400 °C.[51] In this case, the detachment and migration of metal sites are driven by thermal energy. A short distance between the bulk metal and the support would reduce the migration resistance and promote the dispersion of metal sites. Thus, the size of the bulk metal should as small as possible, usually <10 nm. Whether for the gas-assisted CVD strategy or the encapsulation−transformation strategy, the detachment and migration are only important steps for motivating the top-down transformation, while the capturing step of detached metal sites determines the density of the metal site on the support. Once the capturing sites are all occupied by isolated metal sites, the top-down transformation will stop. This highlights that we could increase the metal loading by increasing the density of capturing sites, such as doped nitrogen or vacancies, on the support.

Compared with thermochemical methods, electrochemical methods are harmless to the environment, and they are normally operated with simple two- or three-electrode systems under mild conditions. Notably, certain conditions should be avoided in specific electrochemical reactions. When Pt foil or wire is used as the counter electrode, the potential anodic oxidation will seriously affect the accurate measurement of ORR or HER due to the fact that the dissolved Pt ions can be electrodeposited onto the side of the working electrode, leading to false activity.[52] The researchers reached a consensus that a Pt electrode should be strictly prohibited during electrochemical HER or ORR, and a more inert graphite rod or titanium foil electrode should be used instead. Attention should be paid to avoid these interference factors, and efficient SACs can also be prepared by the electrochemical method. Luo and coauthors synthesized Pt single atoms located on a CoP-based nanotube array catalyst by using potential-cycling methods.[53] Such a binder-free catalyst can easily reach centimeter-scale level and scalability. When using this catalyst as the cathode for HER, the performance is comparable to that of commercial Pt/C at low and high current densities.

2.2. Increasing the Utilization of Metal Sites

The electrocatalytic reaction usually occurs on the three-phase interface consisting of active site, electrolyte, and reacting gas (O_2, CO_2, or H_2), which means that only the electrolyte accessible metal sites could participate in the reaction and serve as real active sites. Currently, the topic of "the utilization

https://doi.org/10.1021/jacsau.3c00001
JACS Au 2023, 3, 736−755

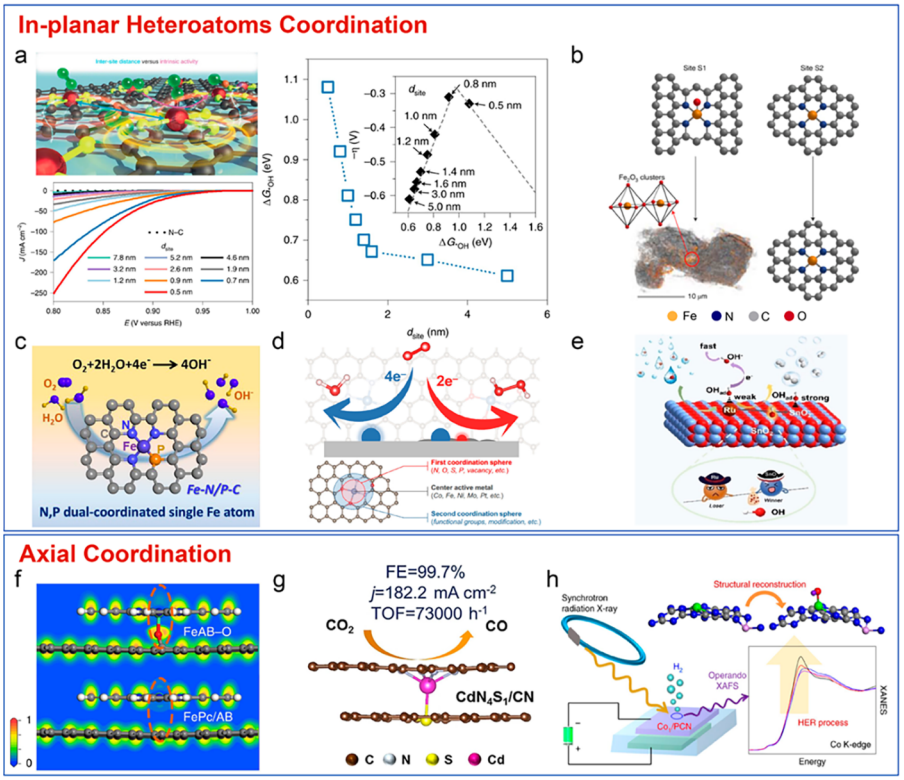

Figure 3. (a) Linear sweep voltammograms of the Fe SACs with different d_{site} values and the d_{site}-dependent ΔG_{*OH} obtained by DFT calculations. (Inset) Volcano plot of calculated overpotentials for the ORR against ΔG_{*OH}. Adapted with permission from ref 58. Copyright 2021 Springer Nature. (b) Fe−N−C catalysts initially comprising two distinct FeN_x sites (S1, FeN_4C_{10}; S2, FeN_4C_{10}) that degrade via the transformation of S1 into iron oxides while the structure and number of S2 is unmodified. Adapted with permission from ref 59. Copyright 2021 Springer Nature. (c) Schematic of N,P dual-coordinated Fe atom catalyst for ORR. Adapted with permission from ref 61. Copyright 2020 American Chemical Society. (d) Schematic of SACs, highlighting the first and second coordination spheres and center active metal. Adapted with permission from ref 63. Copyright 2021 American Chemical Society. (e) Schematic of Ru SACs with low OH_{ad} poisoning effect by the competition adsorption strategy. Adapted with permission from ref 64. Copyright 2022 Wiley-VCH. (f) Electron localization functions on FeAB-O and FePc/AB. Adapted with permission from ref 66. Copyright 2020 Springer Nature. (g) Cd SACs with optimized CdN_4S_1 moiety for CO_2 reduction. Adapted with permission from ref 67. Copyright 2021 Wiley-VCH. (h) Monitoring atomic and electronic structure changes on the Co_1/PCN. Adapted with permission from ref 68. Copyright 2019 Springer Nature.

rate of metal sites" is rarely of concern, and most of the SACs could not realize the full utilization of the metal sites. Methodologies for identifying and increasing the utilization rate of metal sites are challenging but essential.

Generally, a SAC with a high metal loading usually possesses a high surface area, and the isolated metal sites mainly are located at the surface of the micropores. To realize the high utilization of micropores, the support should exhibit good hydrophility and the particle size should not be too big. Wu and coauthors synthesized ZIF-derived Fe−N−C catalysts with particle sizes varying from 20 to 1000 nm and found that the ideal particle size for ORR is 50 nm.[40] With the increase of particle size, the Brunauer−Emmett−Teller (BET) surface area, electrochemical accessible surface area (EASA), and ORR activity of the catalysts decreased simultaneously, suggesting that the inner micropores in the big particles could not be utilized efficiently. Introducing appropriate meso/macropores to the support could also increase the utilization of metal sites by promoting the mass transport. Shui and coauthors employed SiO_2 as a template to construct a ZIF-derived Fe−N−C catalyst with concave morphology, which significantly promoted the mesoporosity and the exposing of active sites (Figure 2c).[54] A hollow structure could also enhance the mass transport and atomic utilization. Lou and coauthors synthesized a fine hollow carbon sphere first and then used a CVD-assisted strategy to construct a high-density Ni single-atom catalyst. They used the CdS balls covered with 3-amino-phenol/formaldehyde resin as precursors, and then gas-migrated Ni single atoms diffused on the exterior surface.[56] After severe steps to remove the original CdS framework, the carbon spheres doped with a high-density Ni single atom were obtained. Nanoframe structures are also efficient strategies to increase the utilization of metal sites. Li and coauthors constructed a three-dimensional open nano-netcage electrocatalyst by employing a dispersing−etching−holing strategy. The porous nano-netcage achieves a high exposure of active sites and a three-dimensional accessibility for substrate molecules, as well as a high performance for overall water electrolysis over a broad pH range. Besides tuning the morphology and porous structure of the support, rationally arranging the metal sites at the surface of the support particle could also increase the utilization of active sites. Jia and coauthors implemented CVD to synthesize an Fe−N−C catalyst by flowing iron chloride vapor over a Zn−N−C substrate at 750 °C (Figure 2d).[55] All $Fe-N_4$ sites formed via this approach are gas phase and electrochemically accessible. Importantly, this work sets an example for us to precisely identify the loading and utilization of metal sites by combining the electrochemical molecular probe and physical characterization techniques.

https://doi.org/10.1021/jacsau.3c00001
JACS Au 2023, 3, 736−755

3. INTRINSIC ACTIVITY OF SINGLE SITE

Although the single metal sites show excellent intrinsic activities for various electrochemical reactions, their electronic structures are not perfect, locating at either the left or the right of the volcano peak. Relative to the well-developed methodologies for increasing the active site density, the development of synthesis methods for tuning the electronic structure of the single metal site is immature, and there are plenty of opportunities to achieve great breakthroughs. Currently, extra heteroatoms (P, S, O, etc.) adjacent to the metal site or at the axial of the metal site have proved to be effective to tune the microenvironment of the single metal site. However, it is challenging to precisely control their specific location and content. Rationally designing the atomic ratio and position of heteroatoms in the precursor by choosing appropriate organic ligands is important and promising. Moreover, exploring new elements beyond P, S, and O may also bring surprises. The most challenging thing is to tune the electronic structure of the metal site continuously, which could not only increase the intrinsic activity of the metal site to the volcano peak but also promote the theoretical study. Another promising approach is introducing a second metal species to construct bimetallic synergetic sites (including dual-atom sites (DACs) and dual hybrid sites). Bimetallic synergetic sites are more than a simple doubling of two single metal species but rather have a synergistic effect of "1 + 1 > 2". However, the research of the bimetallic synergetic site catalysts is still in its infancy and faces a series of challenges, including the construction of bimetallic synergetic sites, accurate characterization of the structure, and elucidation of synergistic effects.

3.1. In-Plane Heteroatom Coordination

In-plane heteroatom modulation is the most commonly used method to tune the electronic structure of the metal active sites for various electrochemical catalytic reactions. Among the heteroatoms, nitrogen atom is the most common choice to coordinate with ma etal center. Chen and coauthors reported a trifunctional catalyst with Fe−N_4 as the active sites for ORR/OER/HER, which indicated that Fe−N_4 sites are capable of various electrochemical reactions.[57] When the distance between two single atoms gradually shortens, how far will electronic interaction occur between them? Yu and coauthors discovered the answer that, when the distance between the two individual Fe−N_4 sites is <1.2 nm, the strong interaction between the adjacent parts will alter the electronic structure (Figure 3a).[58] The improvement in site activity continues until the adjacent Fe−N_4 is as close as ∼0.7 nm, below which the performance is slowly weakened. Although Fe−N_x sites are considered a promising alternative to a noble metal catalyst, the Fe−N_x sites can also be divided into different moieties. Jaouen and coauthors identified the Fe−N−C catalyst that comprised two distinct FeN_x sites: the high-spin FeN_4C_{12} moiety and low/intermediate-spin FeN_4C_{10} moiety (Figure 3b).[59] The ORR activity of the FeN_4C_{12} moiety is higher than that of the FeN_4C_{10} moiety. Regulating the coordination atom often directly affects the electronic structure of the central metal, and the change of the oxidation state of the central metal is one of the most obvious indicators. Cheng and coauthors discovered a volcanic relationship between oxidation state and HER activity based on osmium (Os) SACs.[60] A series of Os SACs with different oxidation states were synthesized by modifying the coordination environments, including Os−N_3S_1, Os−N_4, Os−S_6, Os−C_3, and Os−C_4S_2. They found that the Os−N_3S_1 with a moderate oxidation state (+1.3) possessed the best catalytic performance for HER. Further density functional theory (DFT) calculations proved that the oxidation state mainly adjusts the energy level of the d-orbital to affect the absorption and desorption process. Other heteroatoms (including S, P, and O) directly coordinating with the center metal can also affect the electronic structure of the active sites. Chen and coauthors synthesized and measured the activity of nitrogen and phosphorus co-coordination iron active site (Fe−N/P−C) carbon nanosheets.[61] The N and P dual-coordinated Fe sites were favorable for the adsorption/desorption of the oxygen intermediate, resulting in facilitation of the catalytic oxygen reduction activity (Figure 3c). The S/O co-coordination structure can also optimize the catalytic performance of the materials by regulating the planar electronic structure. Qin and coauthors synthesized a multilayer porous Mo-SAC with two S and two O atoms (Mo−O_2S_2−C) co-coordinated.[62] The S/O co-coordinated structure effectively optimized the adsorption energy of $4e^-$ ORR intermediates at the Mo site, thus significantly improving the catalytic performance. The selectivity of the catalyst can be controlled by adjusting the molecular-level structure of the SACs, including the first coordination sphere (ligands with metal coordination) and the second coordination sphere (functional groups on the host carbon matrix). Qiao and coauthors modulated the selectivity by changing the actual active site (from the central Co atom to the C atom adjacent to O in the second coordination region). In this way, $4e^-$ or $2e^-$ ORR occurs through the adsorption of different electronic structures and intermediates caused by structural and spatial changes in a particular metal center (Figure 3d).[63] In some special cases, proper adjustment of the coordination environment can also play a protective role in preventing the central metal from being poisoned. The strong binding of Ru−OH_{ad} decreases the rate of OH_{ad} transfer. Feng and coauthors introduced the Ru single atom loaded in SnO_2 by replacing the reaction between Ru^{3+} and Sn^{2+} as the HER catalyst (Figure 3e).[64] The basic SnO_2 has excellent absorption of OH_{ad} that can compete with absorbing OH_{ad} with Ru to lower the coverage degree on the Ru single atom. The adjustment of the coordination environment can not only change the kind of coordination atoms but also change the vacancies around the metal center. Bao and coauthors reported that a Ru single-atom catalyst with neighboring Co^{2+} vacancies based on $Co(OH)_2$ shows 4.73 times activity in OER performance compared to that of a catalyst without Co^{2+} vacancies.[65] The result of DFT calculations manifested that with Co^{2+} vacancies *OOH intermediates can form a hydrogen bond with the neighboring O atom, which tunes the absorption configuration of *OOH and lowers the energy barrier of OER.

3.2. Axial Coordination

Apart from tuning the in-plane coordination atoms, there is also an axial coordination regulation for the metal centers.[69] As an example to help with understanding, the M−N_4 structure was considered as the active site of the metal phthalocyanine (MPc) complexes, but the electron distribution of the M−N_4 structure is plane symmetrical. To break the symmetry of the electron distribution, axial coordination is usually considered. Breaking the symmetry of the electronic density would be an effective way to facilitate the oxygen adsorption or activation. Liu and coauthors reported FePc complexes coordinated with the oxidized carbon support (Figure 3f).[66] An axial Fe−O

https://doi.org/10.1021/jacsau.3c00001
JACS Au 2023, 3, 736−755

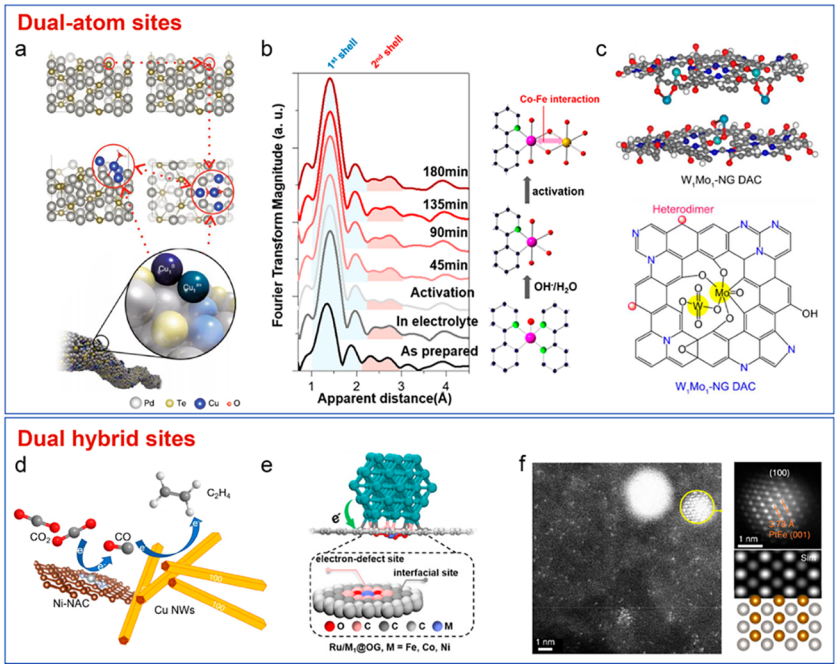

Figure 4. (a) Depicted structures for Cu atom pair anchored on $Pd_{10}Te_3$ nanowires. Adapted with permission from ref 73. Copyright 2019 Springer Nature. (b) Fourier transform of Co K-edge extended X-ray absorption fine structure (EXAFS) spectra for Co−N−C and the formation of Co−Fe double-atom catalyst. Adapted with permission from ref 76. Copyright 2019 American Chemical Society. (c) Schematic illustration of the W_1Mo_1−NG DAC catalyst. Adapted with permission from ref 78. Copyright 2020 AAAS. (d) Hybrid catalyst with Ni single atom and Cu nanowires for CO_2 reduction to ethylene. Adapted with permission from ref 79. Copyright 2022 American Chemical Society. (e) Atomic structures of Ru_{55} supported on O-doped graphene with dispersed metal atoms. Adapted with permission from ref 80. Copyright 2021 Wiley-VCH. (f) HAADF-STEM (high-angle annular dark field scanning transmission electron microscopy) of the hybrid Pt−Fe−N−C catalyst with a dispersed single atom and an individual small nanoparticle with a simulated STEM image and atomic models along the [100] zone axis. Adapted with permission from ref 81. Copyright 2022 Springer Nature.

coordination-induced electronic location approach to facilitate the oxygen activation thus improved the ORR performance. Theoretical calculations found that the axial Fe−O coordination induces the electronic localization among the O−FeN_4 sites to facilitate oxygen adsorption and activation. In addition to the axial Fe−O coordination, other metal active sites with other heteroatoms also have been reported. Peng and coauthors reported a matrix activation combined with the controlled-induction strategy to modify the planar CoN_4 site by axial coordination of Co−S (CoN_4−S_1) for ORR.[70] For comparation, the authors also constructed a CoN_4 site by axial coordination of Co−N (CoN_4−N_1). In this system, the CoN_4−S_1 site shows more capacity for the adsorption and activation of oxygen than that of CoN_4−N_1, which finally reduced the magnitude of the potential-determining step (O_2* → OOH*). Huang and Tang suggested that the axial −NH_2 ligand could promote the ORR activity of the FeN_4 site via weakening the adsorption of oxygen in FeN_4−Ls.[71] Theoretical calculations can also guide the preparation of axially coordinated single-atom catalysts. Han and coauthors found that the cadmium (Cd) single atom can not only decrease the free energy barrier for CO_2 reduction but also suppress the HER (Figure 3g).[67] They synthesized an optimized CdN_4 site with axial coordination of Cd−S, and such a catalyst showed high faradaic efficiency of CO with high turnover frequency. For the same active center, different axial ligands have different ligand effects. The catalytic activity was always affected by the significant axial-ligand effects. Wang and coauthors developed a facile irradiation−impregnation procedure to introduce various halogen atom and hydroxy (−F, −Cl, −Br, −I, and −OH) on the para-position of the Pt single atom located on the NiFe-layered double hydroxide.[72] They calculated and analyzed the effect of the different axial ligands of Pt in the absorption and desorption of H* and finally attributed the influence factor to the average energy levels of the Pt d-orbitals. Among them, Cl−Pt/NiFe-LDH reveals a lower cell voltage (1.87 V) than Ir/C_2 (1.99 V) at a current density of 1 A/cm^2 based on a membrane electrode assembly (MEA) electrolyzer. With the deepening of research, researchers not only pay attention to the structure and coordination environment of the active center of the catalyst before the reaction but also gradually begin to study the dynamic changes of the structure during the reaction. Wei and coauthors reported the dynamic active-site structure of a uniform cobalt single-site (Co−N_4) catalyst during the electrocatalytic alkaline HER by using operando X-ray absorption fine structure (XAFS) (Figure 3h).[68] The operando XAFS combined with Fourier transform infrared (FTIR) and theoretical simulations revealed that the isolated Co−N_4 sites bonded with the electrolyte hydroxide to form a high-valence HO−Co−N_2 moiety. Theoretical simulations further support this structural evolution and also reveal that the high-valence Co sites are responsible for the electrocatalytic performance.

3.3. Bimetallic Synergetic Sites

The electrochemical reactions usually involve multiple elementary reactions and intermediates. The adsorption of intermediates on the active site should be neither too strong nor too weak. However, the adsorption energies of various intermediates on a given single metal site are different and usually follow a scaling relationship, which limits the intrinsic

https://doi.org/10.1021/jacsau.3c00001
JACS Au 2023, 3, 736−755

activity of the single metal site and determines the peak position of the volcano. Although increasing the density and/or intrinsic activity of isolated metal sites could effectively improve the activity of SACs, they do not change the reaction pathways and thus seem to be somewhat powerless to further increase the activity of SACs. The electronic interaction and collaboration between neighboring metal sites makes it possible to design a new reaction mechanism, which allows the different reaction steps to occur on different metal sites, offering great potential in breaking the traditional scaling relationships. In this regard, constructing bimetallic synergetic sites (including DACs and dual hybrid sites) is a promising direction. DACs are more than a simple doubling of two single metal atoms and may have a synergistic effect of "1 + 1 > 2". Similar to the single metal site, the electronic structure of a nanoparticle with controllable crystal face and size also shows good flexibility, but the catalytic properties of the nanocrystal are usually significant versus those of the single metal site. Combining the unique properties and realizing the synergetic catalysis of nanoparticles and single-atom sites may open a new era of electrocatalysis. Introducing extra electronic field, magnetic field, or light to the electrocatalytic system may also change the reaction mechanism, representing a new research topic.

3.3.1. Dual-Atom Sites. Dual-atom sites can be divided into two types: homonuclear and heteronuclear. Different dual-atom structures are designed according to different reaction systems. Chen and coauthors reported an atom-pair catalyst featuring two adjacent copper atoms for the CO_2 reduction (Figure 4a).[73] The atom pair was detected as a $Cu_1^0-Cu_1^{x+}$ pair structure with Cu_1^{x+} adsorbing H_2O and the adjacent Cu_1^0 adsorbing CO_2, which thereby facilitated CO_2 activation synergistically. Zhou and coauthors also reported another homonuclear dual atom as Ag_2/graphene, featuring a well-defined AgN_3-AgN_3 active site.[74] The theoretical calculations can be used for the metal screening and activity prediction of DAC catalysts. Lee and coauthors calculated the formation energies and other reaction variables for different metals (including Fe, Co, Mn, Cu, and Ni) loaded on the N-doped carbon (active structure: $M_1N_3-M_2N_3$).[75] The DFT results predict that Ni−Co dual atoms with a special Ni−Co synergistic effect will get the highest activity for HER in both alkaline and acidic conditions. Then they used the self-polymerization of dopamine to capture the Ni and Co ions, and the Ni−Co dimer was obtained by the following pyrolysis step. The obtained Ni−Co dimer exhibits exceptional pH-universal HER activity, indicating that their DFT prediction supports the experimental results. The preparation of diatomic sites can be obtained simultaneously in situ, or a precatalyst can be prepared first and then the dimer can be obtained. The diatomic sites have synergistic effects, and the role of the individual atoms are also different. Hu and coauthors ingeniously transformed a single-atom Co precatalyst into a Co−Fe double-atom catalyst by using an electrochemical activation of Co species in Fe-containing electrolyte (Figure 4b).[76] The operando X-ray absorption spectroscopy (XAS) provided in depth proof that the structure changes of the Co−N−C moiety occurred after immersion in the alkaline electrolyte and then the Fe species was added during the activation process, resulting in a double-atom Co−Fe moiety. Compared to Co−N−C, Fe is essential for the boosted OER activity of Co−Fe−N−C. Such a double-atom catalyst showed one of the highest turnover frequencies (TOF) among the nonprecious OER catalysts. Li and coauthors reported that the introduction of Mo to the FeN_x configuration could optimize the absorption−desorption behavior of ORR intermediates in the $FeMoN_6$ active moiety, and the cracking of O−O bonds is much more facile on the Fe−Mo atomic-pair site.[77] At present, the $M_1N_3-M_2N_3$ structure is common as the active site for the diatomic catalyst, but other heteroatoms can also be used to anchor the heterodimer. As shown in Figure 4c, Fan and coauthors used a controllable self-assembly and nitridation process to fabricate a dual-atom catalyst featuring an O-coordinated W−Mo heterodimer anchored in nitrogen-doped graphene (W_1Mo_1−NG).[78] The stability and fine distribution of the dual atom were attributed to the O-bridged W−Mo atoms in NG vacancies through the W−O−Mo−O−C configuration. This dual atom showed high activity and stability for HER in a pH-universal electrolyte, and the electron delocalization of the W−O−Mo−O−C configuration possessed superior adsorption strength of H; thus, the HER kinetics can be boosted. Adjusting the local configuration of the atomic catalyst is the key to improving the ORR performance of the catalyst. Instead of the most reported single or diatomic configurations, Fan and coauthors developed a novel three-atom catalyst consisting of the Co−Co and Fe sites of atomic dispersion and nitrogen coordination on the hollow carbon nanocages (Co_2/Fe−N@CHC) graft of carbon nanotubes.[26] The regulated electronic structure of the Fe center reduces the binding energy to oxygen-containing intermediates in the rate-determining step and thus increases the catalytic activity of ORR.

3.3.2. Dual Hybrid Sites. In some special catalytic systems, the catalysis of nanoparticles cannot be replaced by single atoms. In complex tandem reactions (e.g., reduction of CO_2 to C_2 products), a loaded metal catalyst with a single specific active site structure is probably insufficient to provide optimal catalytic reactivity for all steps of a multistep reaction process. Therefore, researchers have solved this problem by synthesizing a tandem catalyst with a dual hybrid site structure. Zhang and coauthors reported a hybrid catalyst by coupling a Ni single atom with a nanoscale Cu component for CO_2 reduction to ethylene (Figure 4d).[79] Among the hybrid catalysts, high-surface-area, ordered mesoporous carbon loaded with a Ni single atom enables the high-rate and selective conversion of CO_2 to CO, while the nanoscale Cu nanowires are capable of the C−C coupling to the C_2H_4 product. Su and coauthors investigated a dual functional site tandem catalyst (Ru_1Ni/CeO_2) containing Ru single atoms and Ni nanoparticles,[82] where CeO_2 nanorods act as a support and provide a large number of oxygen vacancies to prevent the aggregation of Ru single atoms during the reaction. Ru single atoms are quite active in the process of CO_2RR and efficiently convert CO_2 to CO in the Ru active site. The low binding capacity of Ru single atoms to CO* ensures that no hydrogen precipitation occurs during the subsequent reaction. Meanwhile, the short distance between Ru and Ni with competitive adsorption leads to the preferential dissociation of CO_2 to CO at the Ru_1 site. Subsequently, the Ni site converts CO to *CHO by absorbing CO and thus generates methane. In the synergetic effect of the diatomic sites, it often shows the redistribution of electrons, resulting in one electron-rich side and the other electron-deficient side. Liu and coauthors constructed a composite nanoreactor containing single-atom Ru nanoparticles and carbon substrate by using Fe, Co, or Ni doping of O-doped graphene and taking it as a carrier to load

https://doi.org/10.1021/jacsau.3c00001
JACS Au 2023, 3, 736−755

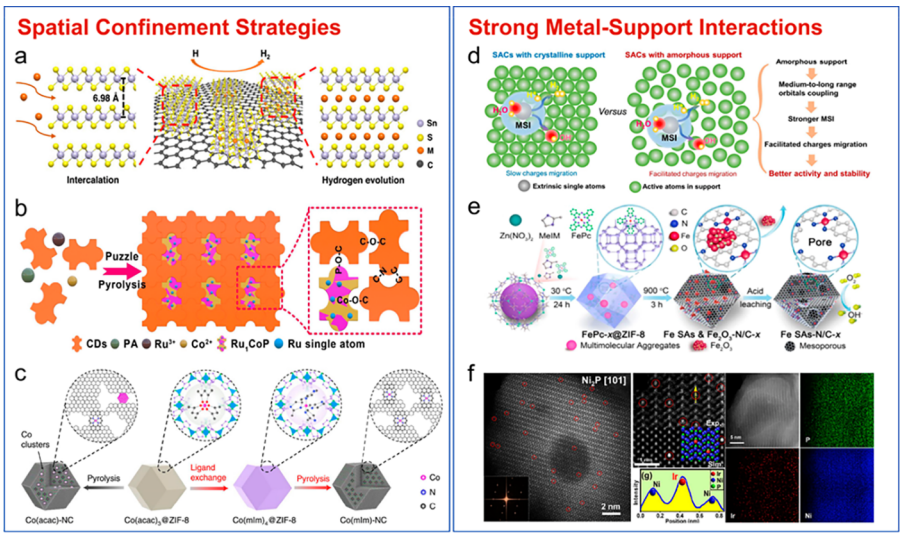

Figure 5. (a) Schematic illustration of the intercalation of layered SnS_2. Adapted with permission from ref 86. Copyright 2022 Springer Nature. (b) Formation of Ru_1CoP/CDs. Adapted with permission from ref 87. Copyright 2021 Wiley-VCH. (c) Two-step encapsulation and ligand-exchange approach effectively introducing CoN_4 complexes into the ZIF-8 micropores. Subsequent one-step pyrolysis produces atomic CoN_4 sites dispersed into porous carbon. Adapted with permission from ref 90. Copyright 2020 Springer Nature. (d) Schematic description of the reaction pathways at the atomic interface of amorphous and crystalline catalysts for alkaline HER electrocatalysis. Adapted with permission from ref 93. Copyright 2022 Wiley-VCH. (e) Schematic illustration for the preparation of Fe SAs-N/C-x. Adapted with permission from ref 94. Copyright 2018 American Chemical Society. (f) Atomic structure recognition of Ir_{SA}-Ni_2P. Adapted with permission from ref 95. Copyright 2021 American Chemical Society.

Ru nanoparticles (Figure 4e).[80] DFT calculations reveal that the single atom led to the redistribution of the surface charge of O-doped graphene, which makes the neighboring C atoms electron-deficient and thus enhances the electron transfer from the Ru nanoparticles to the carbon support. Such a hybrid catalyst shows outstanding HER performance compared to other reported electrocatalysts. In addition, Yang and coauthors explored the effect of electronic structures by introducing the single-atom Ir into Co_3O_4(Ir−Co_3O_4).[83] On the basis of in situ Raman spectroscopy, they prove that the redistribution of electrons between Co and Ir leads to the electron-deficient Co and electron-rich Ir, allowing the faster transfer rate of electrons, especially in the translation of *O to *OOH, which only has a 1.71 eV energy barrier, and enhancing the high activity and stability of OER. In addition to the role of single atoms, intermetallic compounds can also promote the ORR reaction. Shao and coauthors have developed a novel composite catalyst (Pt−Fe−N−C) (Figure 4f).[81] The nitrogen-doped carbon support contains numerous and uniformly dispersed platinum and iron single atoms, accompanied by 2−3 nm Pt−Fe alloy particles. The increased density of active sites in the composite structure shows better performance in the fuel cell test. Theoretical simulations demonstrated that Pt−N_1C_3, Fe−N_1C_3, and PtFe@Pt are indispensable and have great contributions to ORR activity. The single-atom alloy catalyst can greatly increase the density of the metal active sites while considering their synergistic effects. Hu and coauthors reported an HER catalyst using porous $Ni(OH)_2$ nanosheets with Pt loading and then annealing the previous catalyst to get a NiPt alloy catalyst.[84] The X-ray powder diffraction (XRD) spectra show the difference of Ni 2p and Pt 4s between Pt−$Ni(OH)_2$ and the NiPt alloy, which reveals a lower oxidation state of Pt single atom in NiPt. The new Ni−Pt bridge sites provide a low H binding energy, and Ni−Ni bright sites can adsorb H_2O in the alkaline condition. Consequently, the NiPt catalyst has a low overpotential (18 mV) at 10 mA/cm^2.

4. STABILITY OF SACS

The concept of single-atom catalysts is relatively new, and most of the research efforts focus on increasing the activity. With the rapid development of SACs, the activities of some SACs have already met the requirement of commercialization, and the inferior stability is growing as the main obstacle that limits the practical application of SACs. The inferior stability seems like a destiny of SACs, as the single metal sites possess high surface energy and tend to transform into the thermally stable metal clusters. Single-atom catalysts optimize the utilization of metal atoms by exposing the catalytic sites with maximum efficiency, and the unique coordination environment allows them to exhibit unique electronic structure−properties and strong metal−support interactions. The interaction and coordination between the single atom and the support are crucial factors affecting the mobility of the single atom. Once the interaction between the isolated metal site and the substrate was weakened or even destroyed in the operating conditions, which usually involve acid/alkaline solution, oxidative/reductive potential, and destructive radicals, the isolated metal sites would dissolve or aggregate spontaneously. Constructing strong metal−support interaction, which is stable under operating conditions, is the key principle to enhance the stability. To this end, great efforts should be devoted to study the specific deactivation mechanism of SACs under operating conditions. The interaction between the single atoms and the support is enhanced by strategies such as spatial confinement and strong metal−support interactions. In the next section, these strategies will be summarized.

4.1. Spatial Confinement Strategies

Metal single atoms are difficult to exist independently in nature, and they tend to aggregate to form clusters or particles. However, clusters and particles usually have lower catalytic activity in electrocatalysis than single-atom catalysts. Therefore, how can one design many “walls” to separate each individual metal atom and make them move in a specific area?

https://doi.org/10.1021/jacsau.3c00001
JACS Au 2023, 3, 736−755

It is also necessary that these walls provide sufficient electrochemical support for the metal atoms. In general, the spatial confinement strategy is an effective strategy to stabilize single atoms and increase the density of single atoms, including the use of vacancy, interlayer, nanocage, and other carriers to achieve confinement. In electrocatalytic reactions, an increment in the interaction between single atoms and the reactants may cause the aggregation of single atoms by boosting their mobility. The researchers designed cavities in the carrier structure to restrict the movement of single atoms, thus obtaining single-atom catalysts with good stability. Wang and coauthors embedded Ni atoms in graphene shells by polymer nanofiber oxidation and metal surface carbonization treatment.[85] Three-dimensional atom probe tomography was employed to observe the sites of Ni atoms in the vacancies of the graphene shells. The detection results yielded that >80% of the Ni atoms are single atoms. The analysis of the Ni single-atom sites indicated that >95% of the Ni atoms were embedded in the vacant sites of the graphene shell. The catalyst exhibited a Faraday efficiency of ∼93% at a high current for the conversion of CO_2 to CO and exhibited a high turnover frequency (TOF, ∼8 s^{-1}) during 20 h of continuous electrolytic work. Introducing single atoms into the van der Waals gaps of 2D layered materials, instead of them being physically adsorbed or chemically bonded on the surface, can typically improve the stability of the single-atom catalysts. Gong and coauthors reported the layer of SnS_2 on reduced graphene oxide (rGO) introduced with different metal single atoms, which was proved by HAADF-STEM measurements (Figure 5a).[86] Among the different metal precursors, the resulting Pt-SnS_2/rGO catalyst shows superior HER performance and superior long-term stability over 10 000 cycles with the linear sweep voltammetry (LSV) curves remaining unchanged. Another ingenious method is to preferentially confine the local carrier where the single atom is located, so as to stabilize the single atoms. Lu and coauthors used the principle of a jigsaw puzzle to splice the Ru single-atom doped CoP nanosheets with the single-layer carbon dots (Figure 5b).[87] The carbon dot fragments possess abundant functional groups and bind with the CoP nanosheets through P−O−C and Co−O−C coordination; thus, the high density of Ru single atoms can be confined in the jigsaw puzzle. Such a hybrid catalyst showed outstanding stability for HER (2000 cycles during the stability test). Fe−N−C catalysts are the most active nonprecious metal catalysts at present, but they still face the problem of poor stability due to the Fenton effect of the iron ion. A method to improve the stability of the Fe−N−C catalyst is to introduce Fe-free metal and increase the density of active sites of ZIF-derived nitrogen-doped carbon nanocarriers by using a spatial limiting strategy. Wu and coauthors improved the stability of the M−N−C catalyst by improving the stability of the active site of M−N_x−C_y and the corrosion resistance of the carbon support.[47] Manganese doping can significantly improve the degree of graphitization of the carbon materials in the process of high-temperature carbonization, thus improving the stability of the catalyst. For carbon-based SACs, a high graphitization degree could increase the corrosion resistance and stability of the catalyst. However, a high graphitization degree corresponds to a low content of defects and usually leads to a decrease of the active site density. To break this activity−stability trade-off, innovative synthesis techniques allowing the precise removal of useless/harmful defects are highly important.[88,89] Appropriate metal species in the support could serve as a buffer and suppress the structure evolution during the catalytic process, thus enhancing the stability of the catalysts. The activity of Co ion in the Fenton reaction is low (which reduces the rate of free radical formation and the attack of free radical on the catalyst) and significantly enhances the demetallization resistance of Co−N−C. Shao and coauthors fixed the ligand-chelated Co−N_x groups in the micropores of ZIF-8 and utilized the unique hydrocarbon network of ZIF-8 to act as a protective barrier between individual Co atoms, which reduced its mobility and avoided Co agglomeration (Figure 5c).[90] The catalyst was comparable in activity to a similarly synthesized Fe−N−C catalyst, but its durability was improved by 4 times. Chen and coauthors obtained Co−N_5 active sites by anchoring Co single atoms in N-doped hollow carbon spheres.[91] Pyrrole N with strong coordination affinity functioned as the anchoring site for the Co single atom. Surprisingly, the CO current density values and FE_{CO} were essentially constant during 10 h of electrolytic work. Sun and coauthors fabricated N-doped graphene support single Pt atoms by using the ALD technique.[92] These Pt SACs showed significant long-term stability in the HER test without obvious catalytic activity decrease even after 1000 cyclic voltammetry sweeps at fixed potentials. According to Bader charge analysis, 0.25 e^- charge transfer from Pt atom to N-doped graphene occurs on the Pt single atom, while the charge transfer between the Pt atom and the original graphene is almost negligible. These results indicate that the formation of this highly stable SAC is attributed to the strong interaction between the Pt single atom and the adjacent N atom.

4.2. Strong Metal−Support Interactions

Besides carbon-based materials being used as carriers for single-atom catalysts, metal carriers are emerging on the horizon for researchers. The interactions between single atoms and metal carriers are exploited to prevent the aggregation of single atoms in electrocatalytic reactions. The choice of carriers with a strong metal support enhances the dispersion of atoms and consequently the stability of the catalysts. Zheng and coauthors suggested the presence of CeO_2 nanorods as carriers for Cu single atoms; the strong interaction between Cu and CeO_2 ensured that the aggregation of Cu single atoms was reduced under high-temperature reactions.[96] Theoretical calculations revealed that, at CeO_2(110), Cu^{2+} replaces Ce^{4+} at the first oxygen vacancy and Cu single atoms attain the optimal stable structure when there are three oxygen vacancies formed. The Cu-substituted CeO_2 exhibited a strong adsorption capacity for CO_2 with increasing temperature. The Faraday efficiency of 58% conversion of CO_2 to CH_4 was tested in an H-type electrochemical cell, and the conversion efficiency of >40% was maintained for >130 min of continuous electrolytic operation. The substrates of an oxygen-based chemical compound can be classified into crystalline and amorphous. Amorphous supports have more defects and more kinds of anchor sites, which can often achieve better catalytic performance. Lee and coauthors researched the difference of induced metal−support interaction (MSI) between the amorphous and crystalline supports. They synthesized single-atom Ru on amorphous NiCoOOH(Ru−a-CoNi) and on crystalline NiCoOOH(Ru−c-CoNi) in different ways (Figure 5d).[93] Due to the stronger MSI, Ru−a-CoNi alleviates the affinity of O toward H* and leads to fast HER kinetics and high stability. The electrochemical test results show that Ru−a-

https://doi.org/10.1021/jacsau.3c00001
JACS Au 2023, 3, 736−755

CoNi has steadier HER activity at −20 mA/cm^2 than Ru−c-CoNi for 50 h. Selective C−N bond cleavage at the adjacent Fe−N_4 site was triggered using stratified pores. This edge-bearing Fe−N_4 configuration is key to tuning the N-bonding structure, significantly reducing the overall ORR barrier. Wang and coauthors encapsulated iron phthalocyanine in ZIF-8 to form FePc-x@ZIF-8, which breaks the limiting effect of microcavities and plays a crucial role in edge-site engineering and mesopore construction (Figure 5e).[94] Precisely controlling the coordination environment could also increase the interaction between the metal site and the support. Jaouen and coauthors identified that the FeN_4C_{10} moiety is a durable active site in an acid electrolyte, while the FeN_4C_{12} moiety is nondurable and will convert to Fe_2O_3 clusters during the process.[59] The calculation result reveals that the axial OH ligand on the metal center of Fe−N−C is unfavorable for the catalysts' stability due to much increased H_2O_2 selectivity.[97] Another operation to stabilize the single atom is regulating the synthesis process. Most reported routes tend to directly load the single atom on the basement materials through a replacing reaction, which results in poor long-term catalytic stability. A simple top-down process can avoid this problem. Gu and coauthors reported a Ni_2P catalyst loaded with an Ir single atom (Figure 5f).[95] They heated the precursors of Ir and Ni together with excess P sources, which provided an abundant P environment. After observing the growth of Ir−Ni_2P in detail, they proved that the Ir−O−P bond generated before Ir is loaded on Ni_2P leads to the high stability of the single atoms. The current density only decays 2.1% after 40 h at a constant potential of 1.5 V. The same approach also applies to other single atoms like Au and Rh. However, Liu and coauthors presented another original point that the formation of clusters may not be bad for the catalysts.[98] They used the constant-potential hybrid-solvation dynamic model to evaluate the reversible transformation between Cu single atoms and clusters under realistic reaction conditions. It was revealed that the combination of a single atom and a cluster has high activity to promote CO_2 reduction to ethanol. It will be worthwhile to do more research on the real effect of other clusters.

Besides the metal−support interaction, the structural stability of the support also affects the stability of SACs. The structural damage of the support not only directly leads to the dissolution of metal sites but also changes the electronic structure of the metal site and thus decreases their intrinsic activity. Highly ordered graphitized carbon materials are more stable, but they usually result in low surface area and insufficient porosity, which makes them unfavorable for mass transfer in the cathode. Balancing graphitization and porosity of the catalyst carbon support is very important to obtain stable and efficient support materials. Wu and coauthors compared the catalytic capacity of different metals (including iron, cobalt, nickel, and manganese) to graphitize carbon under high-temperature calcination and found that only manganese could catalyze the formation of extremely graphitized carbon materials at 1100 °C.[89] Compared with the traditional graphitized carbon synthesis process (3000 °C), this carbon base material has high catalytic activity and stability. Other ways to use a multicarbon support or in situ encapsulation of N-doped carbon materials to form a stable support can improve the stability of the substrate.

5. SITE STRUCTURE AND REACTION MECHANISM

With the increasing demand for structural knowledge of single-atom catalysts, effective probing of catalyst surface states such as defects, atomic reconfiguration, elemental arrangements, and molecular adsorption is an indispensable step to improve catalyst performance. Meanwhile, precise insight into the catalyst structure allows a more practical construction of the conformation relationship between catalyst structure and performance. To achieve this goal, a variety of characterization instruments have sprung up.[99] Traditional ex situ characterization methods reflect the state of catalysts before and after reaction, whereas catalytic reactions not only require steady state but also focus on transient reactions, such as the utilization of in situ characterization methods to detect in real time the atomic structure change of the catalyst, intermediate change of adsorbed molecules into catalytic products, chemical state of the catalyst, oxidation or reduction, and ligand atom shift. This series of reaction intermediate processes is crucial to study the mechanism of catalytic reactions and the choice of catalysts that are employed. The theoretical calculation is enhanced by a detailed understanding of the catalyst structure, which leads to a more realistic, rational, and effective theoretical structure.[100] It plays an irreplaceable role in facilitating the subsequent catalyst design, thus forming a virtuous circle.

5.1. Ex Situ Characterizations

Electron microscopy techniques are particularly suitable for determining the presence of individual metal atoms and their location in the surface structure of the carrier in combination with their spatial distribution, which is essential for the development and optimization of methods for the synthesis of single-atom catalysts. The STEM provides a way to determine whether the high loadings are derived from metals or nanoparticles. Li and coauthors developed a high-density Ir-loaded (18 wt %) catalyst based on NiO. With the help of ex situ characterization, the STEM figure shows the average distribution of Ir single atoms, and the X-ray absorption spectroscopy (XAS) of Ir shows that the double peaks belong to Ir^{4+} and Ir^{3+} rather than other nanoparticles.[44] In addition, the synthesized PtZn intermetallic compounds based on the lattice stripes were observed by aberration-corrected STEM (AC-STEM), which also corresponded to the atomic arrangement of the planes in the PtZn crystal structure. It supported the subsequent verification of the conclusion that Ni single atoms were obtained by metal exchange.[101] Although the AC-STEM provides valuable information for the characterization of loaded single-atom catalysts and optimization of their synthesis, the composition of individual metal atoms is still difficult to analyze. A limitation of the electron beam induction effect and detection sensitivity hinders the characterization of single atoms loaded on the surface of high specific surface area carriers.

Extended X-ray absorption fine structure (EXAFS) and X-ray absorption near-edge spectroscopy (XANES) methods are widely utilized for the characterization of loaded metal nanoparticles or clusters. EXAFS spectroscopy to characterize the metal−metal coordination number serves to efficiently determine whether a single-atom catalyst is successfully obtained. Müller and coauthors constructed single-atom Fe sites in MXene two-dimensional materials for the first time.[102] Characterization by XAS spectroscopy revealed that the Fe sites were modified in the lattice in a manner that replaced the

https://doi.org/10.1021/jacsau.3c00001
JACS Au 2023, 3, 736−755

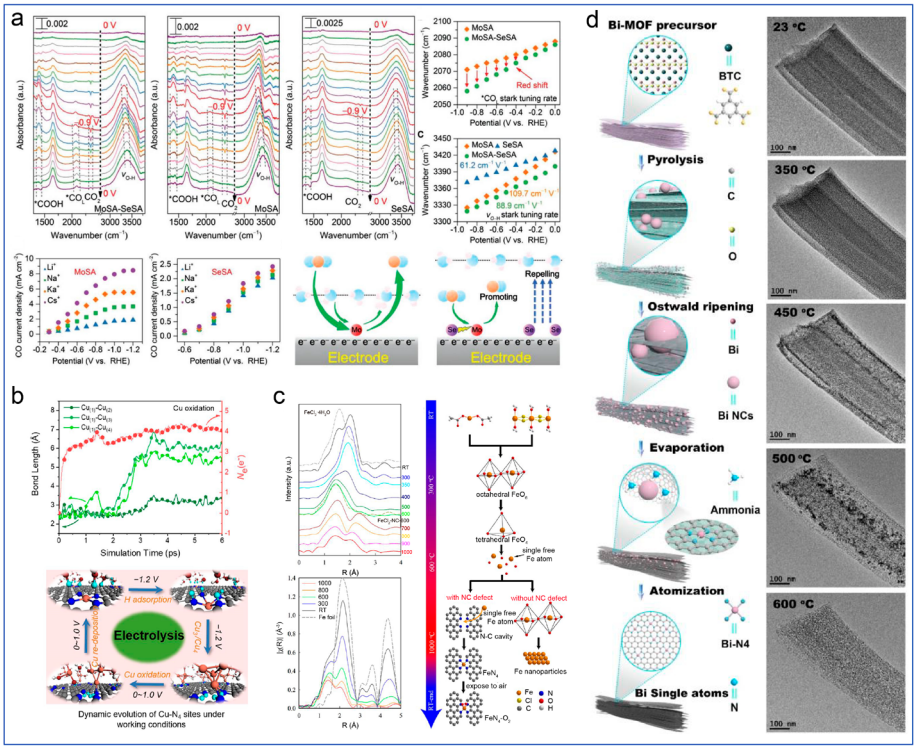

Figure 6. (a) Mechanistic study by ATR-SEIRAS spectra and schematic diagram of the reaction mechanism. Adapted with permission from ref 107. Copyright 2022 Wiley-VCH. (b) Summary illustration of the mechanism of the dynamic reversible transformation of the Cu single-atom cluster catalytic structure under working conditions. Adapted with permission from ref 98. Copyright 2022 American Chemical Society. (c) Schematic illustration of the common pathways up to 600 °C of the thermal evolution of iron compounds during pyrolysis and then diverging pathways at $T \geq$ 600 °C depending on the absence or presence of N−C defects. Adapted with permission from ref 109. Copyright 2020 American Chemical Society. (d) Scheme of the transformation from Bi-MOF (MOF, metal−organic framework) to single Bi atoms and corresponding representative TEM images of Bi-MOF pyrolyzed at different temperatures with the assistance of DCD in situ. Adapted with permission from ref 110. Copyright 2019 American Chemical Society.

Mo sites. Mo_2CT_x:Fe catalysts were synthesized by modifying Fe single-atom sites in two-dimensional Mo_2CT_x molybdenum carbide MXene, and high catalytic activity and selectivity were achieved in the synthesis of H_2O_2 by the ORR. Wang and coauthors fabricated Cu−NC with pyrolysis, and ex situ characterization showed that the atomically dispersed Cu^{2+}−N_4 structure remained unchanged before and after the reaction; however, XANES spectra clearly revealed a potential driving dynamic evolution from Cu^{2+}−N_4 to Cu^{+}−N_3 to HO−Cu^{+}−N_2 under ORR operating conditions. The Cu^{+}/Cu^{2+} ratio appears to rise with increasing applied potential, suggesting that the low-coordinated Cu^{+}−N_3 fraction is the true active site.[103] Jiang and coauthors investigated whether Zn in Zn−N_3−C is in the oxidized state observed by XANES because of its higher near-side absorption energy, while the absence of the Zn−Zn bond was obtained by EXAFS. Further EXAFS fits showed that each Zn atom is coordinated by three N atoms, confirming that Zn−N_3 is the dominant coordination mode in Zn−N_3−C.[104] In EXAFS, metal−metal bonds in the active species are not present. Therefore, in cases where EXAFS data contain a lack of indications of metal−metal bonding, it can be inferred that only single metal atoms are present in the catalyst. However, EXAFS presents two-dimensional details and is not sufficient to determine the three-dimensional structure.

Infrared (IR) spectra allow direct detection of interactions between adsorbed molecules and carrier surfaces, and time- and temperature-resolved Fourier transform infrared spectroscopy enables the detection of catalytic intermediates. By detecting the vibrational frequency and intensity of the model to be analyzed, the properties of the active center with appropriate corrections can be deduced.[105] Han and coauthors observed the asymmetric and symmetric vibrations of the carboxylate anion of In_A/NC in the 1,3,5-H ligand by IR results, which, combined with the symmetric stretching vibrations of proto-H_3BTC and In−O, identified the coordination of BTC with In.[106]

5.2. In Situ Characterizations

The operando characterizations and theoretical simulations play great roles in identifying the active site structure as well as the reaction mechanism. Currently, the electrochemical in situ technique in a three-electrode system is relative mature, but the operando characterizations of the electrochemical devices are still challenging. Advanced operando techniques hold great promise to open the black box of electrochemical devices, prompting the practical application and theoretical study of SACs.

Because molecules are capable of selectively absorbing infrared light at certain wavelengths, this causes oscillations of molecules and leaps in rotational energy levels. Therefore, it is possible to detect the absorption of infrared light for obtaining infrared absorption spectra of substances. Operando attenuated total reflection surface-enhanced infrared absorption spectroscopy (ATR-SEIRAS) identifies the specific reactions of single atoms with intermediates by probing the thermodynamic forces on an atom dynamic of the intermediates. Chen

https://doi.org/10.1021/jacsau.3c00001
JACS Au 2023, 3, 736−755

and coauthors synthesized Mo−Se dual-atom catalysts on hollow nanosheets, which exhibited up to 90% FE_{CO} under continuous electrolysis for 23 h at −0.4 to −0.8 V (Figure 6a).[107] It was observed by operando ATR-SEIRAS that the valence bands of *COOH and CO_2 of Mo single atoms fade away from −0.1 to 0 V, and the *CO valence band exists as a potential backward, indicating the strong adsorption of CO and the possibility of CO poisoning by Mo single atoms. The observation of the O−H valence band in the reaction of Mo single atoms from −0.9 to 0 V indicated high fluctuation, suggesting that the occurrence of hydrogen precipitation reactions during the reduction process may affect the catalytic performance. However, the introduction of Se single atoms was accompanied by a red-shift of the *CO valence band, thus inferring that Se single atoms could attenuate the strong adsorption of CO* on the neighboring Mo single atom through long-range electronic interactions. At the same time, Se single atoms improve the catalytic performance by enhancing the ability of the Mo single atom to repel water molecules. This evidence explains why the introduction of Se single atoms can enhance the catalytic efficiency of CO_2RR. The in situ SR-micro-FTIR technique plays an irreplaceable role while monitoring the real catalytic process. Whether Mo or S is the real active site in MoS_2 2D nanosheets in HER remains a debate. Wei and coauthors designed an HER catalyst MoS_2 with a Co single atom loaded and identified the real active site using in situ SR-micro-FTIR measurement.[108] There is an obvious absorption band with E less than −0.05 V (vs RHE) for the S−H bonds, indicating that the real active site is the S atom magnetized by Co rather than the metal atoms Mo or Co. This also explained the higher activity in MoS_2 with long-range ferromagnetism. In situ diffuse reflectance infrared Fourier transform spectroscopy (DRIFTS) characterizes the intermediates produced in the catalytic process to determine the decisive steps affecting the reaction rate. Su and coauthors reported a dual active site catalyst in tandem (Ru_1Ni/CeO_2) consisting of Ru single atoms and Ni nanoparticles, which is effective in converting CO_2 to CH_4 with ∼90% CO conversion and 99% CH_4 selectivity at 325 °C.[82] The peak intensities of bicarbonate (1640 cm^{-1}), polydentate (1428 cm^{-1}), and monodentate (1509 cm^{-1}) were observed at different temperatures for Ni/CeO_2 under three gases and at 50−350 °C with the temperature increases. The bands of CO* (2022 and 1902 cm^{-1}), *CHO (1746 cm^{-1}), and methane (3016 cm^{-1}) appeared at temperatures above 200 °C. Meanwhile, the bands of HCOO* (2842 and 1349 cm^{-1}) and carboxylate (1270 cm^{-1}) gradually decreased, indicating that CO*, *CHO, and methane were mainly produced by the hydrogenation of HCOO*. It was verified by DFT analysis that the HCOO* reaction pathway of CO_2 methanation indeed occurred on Ni/CeO_2. The reaction process on Ru_1/CeO_2 was the dissociation of CO_2 to CO*, while in Ru_1Ni/CeO_2 the conversion of CO* to methane is possible due to the active site of Ni. The energy band intensities of *CHO and HCOO* increased with time, while the energy band intensity of HCOO* increased faster because the conversion of HCOO* to *CHO is the rate-determining step of the reaction. The intensity of *CHO relative to Ru_1Ni/CeO_2 was significantly higher than that of Ni/CeO_2, which further demonstrated the superior CO_2 activation performance of Ru_1Ni/CeO_2. The accuracy of this reaction mechanism was established by in situ DRIFTS characterization results.

In situ XAFS permits rapid and high-precision analysis of elements, their valence states, and even their respective distributions within single-atom catalysts, which is of crucial importance for insight into the catalytic mechanism.[111] Comprehension of the impact of the catalytic pathway at the atomic level assists researchers in designing single-atom catalysts. During the study, a combination of in situ XAFS and DFT theoretical calculations was analyzed to help researchers interpret the effects of structural and electronic properties of single-atom catalysts in electrocatalytic reactions. Another important function of the in situ characterization technique is observing the dynamic structure of single-atom active sites. Wei and coauthors used in situ XAFS to observe the formation of active $HO−Co_1−N_2$ with a high oxidation state of Co in carbon-based N-doped Co HER catalyst under working conditions, which is consistent with the theoretical investigations about the strong charge transfer. The formation of highly oxidized $HO−Co_1−N_2$ was revealed by DFT analysis of the electronic and geometric structural changes occurring on the Co site, with the favored dynamic H_2O adsorption as $H_2O−(HO−Co_1−N_2)$.[68] Liu and coauthors presented another original point that the formation of clusters may not be bad for the catalysts (Figure 6b).[98] They used the constant-potential hybrid-solvation dynamic model to evaluate the reversible transformation between Cu single atoms and clusters under realistic reaction conditions. It was revealed that the combination of a single atom and a cluster has high activity to promote CO_2 reduction to ethanol. The real effect of other clusters is worthy of more research. Chen and coauthors first synthesized the Pd single-atom catalyst for CO_2RR.[112] To observe the structural changes of Pd/C and Pd−NC during CO_2RR, in situ XAFS analysis of the Pd K-edge was performed in the potential range (0.3 to −0.8 vs RHE). XANES and EXAFS results revealed the formation of PdH at −0.3 vs RHE in Pd/C, and the Pd−Pd bond length increased with increasing potential. The results for DFT analysis for Pd−NC indicated that no PdH was formed during the catalytic reaction and the change in Pd−Pd bond length was negligible. On the basis of the results of in situ XAFS analysis, it is regarded that Pd−NC with $Pd−N_4$ as the activation center possesses good stability in the CO_2RR reaction. Hu and coauthors demonstrated a method of maintaining the active site as a trivalent oxidation state structure of $Fe^{3+}−N−C$ as a CO_2RR catalyst through electronic coupling.[113] The analysis of the in situ XAFS results revealed that the Fe was in the +2 oxidation state in the CO_2RR reaction. In the pulse current experiments, the current density of the Fe in the +2 oxidation state was significantly lower than that of the Fe in the +3 oxidation state. The pyrrole-type ligand is important to retain the Fe site in the +3 oxidation state during CO_2RR, thus maintaining the high activity and stability of the Fe^{3+} site. Xing and coauthors prepared the single-atom catalyst Ru-SSC by a simple pyrolysis method. In situ EXAFS characterization revealed that the in situ generated OH* ligands could modulate the d-orbital electronic structure of Ru, thus optimizing the adsorption energy of Ru on oxygen-containing intermediates.[114] Jia and coauthors revealed by in situ temperature X-ray absorption spectroscopy the evolutionary pathway of the precursor to an ORR-active catalyst composed entirely of single-atom $Fe_1(II)−N_4$ sites (Figure 6c).[109] The $Fe_1(II)−N_4$ site was synthesized by noncontact pyrolysis, in which the Fe precursor does not come into physical contact with the N and C precursors during the pyrolysis process.

https://doi.org/10.1021/jacsau.3c00001
JACS Au 2023, 3, 736−755

In situ Mössbauer spectroscopy is a powerful technique to study the magnetic properties of metal sites, especially the FeN_x sites. Jaouen and coauthors discovered by in situ ^{57}Fe Mössbauer spectroscopy and DFT analysis that Fe−N−C catalysts contain two types of FeN_x sites labeled D1 (quadrupole cleavage doublet (QS) values of 0.9−1.2 mm s^{-1}) and D2 (QS values of 1.8−2.8 mm s^{-1}), which have similar isomeric shifts.[59] They identified D1 to be a high-spin FeN_4C_{12} moiety (S1) and D2 to be a low- or medium-spin FeN_4C_{10} moiety (S2). It was demonstrated in an oxygen-free proton-exchange membrane fuel cell (PEMFC) that part of S1 is stable and reversibly shifts from a high-spin iron state to a high-spin ferrous state between 0.8 and 0.2 V, while the electronic state of S2 is potential-independent. The FeN_4C_{10} moiety is a durable active site in acid electrolyte, while the FeN_4C_{12} moiety is nondurable and will convert to Fe_2O_3 clusters during the process. Employing the in situ ^{57}Fe Mössbauer spectroscopy, Liu and coauthors identified that the N−FeN_4C_{10} moiety is a more active site for ORR. They also proved that the N−FeN_4C_{10} site undergoes geometric and electronic structure evolution during the potential cycling.[115]

In situ transmission electron microscopy (TEM) provides conditions close to the real environment and directly correlates microstructural changes in materials with external signals. In situ TEM carries significance for expanding the experimental methods for materials at the microscopic scale, understanding the nature of various dynamic reactions, and designing and preparing materials with novel properties. In addition, in situ environmental transmission electron microscopy (ETEM) enables real-time observation of chemical reaction kinetic processes at the atomic scale. Li and coauthors fabricated a Bi single-atom catalyst for CO_2RR with a thermal decomposition method (Figure 6d).[110] In situ ETEM at elevated temperatures was employed to study the evolution of Bi-MOF to a Bi single atom. With the increase of temperature, Bi-MOF was gradually pyrolyzed to Bi−NP, and the atomized Bi−NP was subsequently promoted by NH_3 generated from the pyrolysis of dicyandiamide to produce Bi−N_4 active sites with N in the carbon network. In situ ETEM provides a fundamental guiding theory for the study of MOFs to prepare single-atom catalysts with atomically dispersed metal active sites.

It should be noted that the development of in situ characterization techniques is relatively primary at the current time. The experimental results are usually not perfect and rely on the experimental devices and conditions. Testing standards of in situ characterizations should be established to generate reliable results.

6. CONCLUSION AND OUTLOOK

Since the concept of single-atom catalysts was formally proposed in 2011, SACs featuring low cost and high efficiency have emerged as the most promising alternative to traditional precious-metal-based catalysts for various electrochemical reactions. Moreover, the simplified components and unitary site structure of SACs make it possible to uncover the fascinating electrocatalytic mechanism with operando characterization techniques and theoretical simulations. To this day, tremendous efforts have been made to develop advanced SACs with high activity and stability, and great breakthroughs on innovative synthesis methods, structure characterization, and reaction mechanism have been achieved. However, the practical applications of SACs in electrochemical devices have not been realized, and the electrocatalytic mechanism is still unclear. Current understandings about the unique properties of SACs are just the tip of the iceberg, but the further development of SACs seems to encounter a bottleneck. To further dig into the mine of SACs, revolutionary exploration in the following aspects should be executed to break current bottlenecks, which is challenging but essential.

(1) Further increasing the loading of active metal sites. The excellent activity of SACs mainly benefits from the high density of active sites. Although various synthesis methods have been reported to increase the active site density, the current level of metal loading is still far from the theoretical upper limit; thus, increasing the metal loading is still the first choice to break the current activity ceiling of SACs. The preparation of SACs usually involves two steps including the liquid-phase synthesis of precursor and the thermal activation/carbonization, during which competitive side reactions that lead to agglomerations occur and limit the formation of isolated metal sites. In the precursor synthesis step, even trace H_2O or O_2 could lead to the hydrolyzation or oxidization of the metal salt. Limited by the hydrolytic equilibrium, a high concentration of metal salt would be more sensitive to the trace H_2O or O_2, which is the reason that one could not increase the density of isolated metal sites in the precursor by simply increasing the concentration of metal salt. Thus, the trace H_2O in the solvent and even crystal H_2O in the raw materials should be seriously considered. A water-removal treatment before the addition of metal precursor may be helpful. Moreover, we could suppress the hydrolysis by constructing a stronger coordination bond between the metal site and the organic ligands. In the thermal activation/carbonization step, carbon atoms at high temperature could inevitably serve as a reductant to break the bond between metal the sites and the substrate, and the high temperature could also lead to the dissociation and volatilization of nitrogen atoms, which are the main anchor sites of isolated metal atoms. The thermally driven nitrogen loss and carbon activation (as reductant) seem to be inevitable, and they work synergistically to trigger the agglomeration of metal atoms. As a result, although the isolated metal sites in some designed precursors are dense, they could not survive in the heat-treatment step. In this regard, preventing the nitrogen loss and minimizing the time of heat-treatment would be effective. Currently, the heat-treatment process is usually performed in a normal tube furnace with a relatively low heating rate (2−5 °C/min) and long time (1−5 h), and the time that the precursor stays at nthe ontarget temperature interval is very long, which is adverse for retaining isolated metal sites. We highlight that the rapid-heating and instantaneous-carbonization technique based on a novel furnace may bring great breakthroughs. Besides, introducing a nitrogen-rich sacrificial agent upstream of the furnace to continuously provide a nitrogen source to the precursor could also increase the nitrogen anchor sites and thus the isolated metal sites.

(2) Increasing the intrinsic activity of the active site. Although the single metal sites show excellent intrinsic activities for various electrochemical reactions, their electronic structures are not perfect, locating at either the left or the right of the volcano peak. Relative to the well-developed methodologies for increasing the active site density, the development of synthesis methods for tuning the electronic structure of a single metal site is immature, and there are plenty of opportunities to achieve great breakthroughs. Currently, extra heteroatoms (P, S, O, etc.) adjacent to the metal site or at the

https://doi.org/10.1021/jacsau.3c00001
JACS Au 2023, 3, 736−755

axial of the metal site have proved to be effective to tune the microenvironment of the single metal site. However, it is challenging to precisely control their specific location and content. Rationally designing the atomic ratio and position of heteroatoms in the precursor by choosing appropriate organic ligands is important and promising. Moreover, exploring new elements beyond P, S, and O may also bring surprises. The most challenging thing is to tune the electronic structure of the metal site continuously, which could not only increase the intrinsic activity of the metal site to the volcano peak but also promote the theoretical study.

(3) Synergetic catalysis with a new mechanism. The electrochemical reactions usually involve multiple elementary reactions and intermediates. The adsorption of intermediates on the active site should be neither too strong nor too weak. However, the adsorption energies of various intermediates on a given single metal site are different and usually follow a scaling relationship, which limits the intrinsic activity of the single metal site and determines the peak position of the volcano. Although increasing the density and/or intrinsic activity of isolated metal sites could effectively improve the activity of SACs, they do not change the reaction pathways, and thus it seems to be somewhat ineffective to further increase the activity of SACs. The electronic interaction and collaboration between neighboring metal sites make it possible to design a new reaction mechanism, which allows the different reaction steps to occur on different metal sites, offering great potential in breaking the traditional scaling relationships. In this regard, constructing a dual-metal active site is a promising direction. Similar to a single metal site, the electronic structure of a nanocrystal with controllable crystal face and size also shows good flexibility, but the catalytic properties of the nanocrystal are usually significant from that of the single metal site. Combining the unique properties and realizing the synergetic catalysis of a nanocrystal and a single-atom site may open a new era of electrocatalysis. Introducing extra electronic field, magnetic field, or light to the electrocatalytic system may also change the reaction mechanism, representing a new research topic.

(4) Increasing the stability of SACs. The concept of single-atom catalysts is relatively new, and most of the research efforts focus on increasing the activity. With the rapid development of SACs, the activities of some SACs have already met the requirement of commercialization, and the inferior stability is growing as the main obstacle that limits the practical application of SACs. The inferior stability seems like the destiny of SACs, as the single metal sites possess high surface energy and tend to transform into thermally stable metal clusters. Once the interaction between the isolated metal site and the substrate is weakened or even destroyed in the operating conditions, which usually involve acid/alkaline solution, oxidative/reductive potential, and destructive radicals, the isolated metal sites would dissolve or aggregate spontaneously. Constructing strong metal−support interaction that is stable under operating conditions is the key principle to enhance the stability. To this end, great efforts should be devoted to study the specific deactivation mechanism of SACs under operating conditions. Besides the metal−support interaction, the structural stability of the support also affects the stability of SACs. Structural damage of the support not only directly leads to the dissolution of metal sites but also changes the electronic structure of the metal site and thus decreases their intrinsic activity. For carbon-based SACs, a high graphitization degree could increase the corrosion resistance and stability of catalysts. However, a high graphitization degree corresponds to a low content of defects and usually leads to a decrease of the active site density. To break this activity−stability trade-off, innovative synthesis techniques allowing the precise removal of useless/harmful defects are highly important. Appropriate metal species in the support could serve as a buffer and suppress the structure evolution during the catalytic process, thus enhancing the stability of the catalysts.

(5) Designing the porous structure of SACs. Different from the simplified three-electrode system, practical electrochemical devices featuring a high reaction flux and the mass-transport process are critically important. Ideal mass transport not only promotes the utilization of the active site but also increases the stability by timely discharge of the reaction products. Currently, the mass transport is mainly determined by the meso/macropores. Meanwhile, micropores could increase the active site density by providing a high surface area. The rational design of a hierarchical porous structure could combine the advantages of micropore and meso/macropores and is of vital importance for a practical catalyst. The main challenge is to precisely control the ratio and spatial distribution of various pores. Applying the self-assembly technique to the synthesis of a precursor may help to break the current bottleneck. Additionally, MOF and covalent−organic framework (COF) materials with flexible and long-range order structure also provide ideal platforms to precisely control the pore distribution.

In summary, precise synthesis methods should be developed by designing ideal precursors and exploring innovative heat-treatment techniques to break the bottlenecks on further increasing the activity and stability of SACs. The assembling of hierarchical pores is also very important for realizing the application of SACs in practical electrochemical devices. The operando characterizations and theoretical simulations play great roles in identifying the active-site structure as well as the reaction mechanism. Currently, the electrochemical in situ technique in a three-electrode system is relative mature, but the operando characterizations of the electrochemical devices are still challenging. Advanced operando techniques hold great promise to open the black box of electrochemical devices, prompting the practical application and theoretical study of SACs. Finally, large-scale production is also essential for the industrial application of SACs; we should keep an eye on establishing industrial-scale synthesis methods.

AUTHOR INFORMATION

Corresponding Author

Chen Chen − *Engineering Research Center of Advanced Rare Earth Materials, Department of Chemistry, Tsinghua University, Beijing 100084, P. R. China;* orcid.org/0000-0001-5902-3037; Email: cchen@mail.tsinghua.edu.cn

Authors

Jiazhan Li − *Engineering Research Center of Advanced Rare Earth Materials, Department of Chemistry, Tsinghua University, Beijing 100084, P. R. China*

Chang Chen − *Engineering Research Center of Advanced Rare Earth Materials, Department of Chemistry, Tsinghua University, Beijing 100084, P. R. China*

Lekai Xu − *Engineering Research Center of Advanced Rare Earth Materials, Department of Chemistry, Tsinghua*

https://doi.org/10.1021/jacsau.3c00001
JACS Au 2023, 3, 736−755

University, Beijing 100084, P. R. China; orcid.org/0000-0002-5792-9932

Yu Zhang − *Engineering Research Center of Advanced Rare Earth Materials, Department of Chemistry, Tsinghua University, Beijing 100084, P. R. China*

Wei Wei − *Engineering Research Center of Advanced Rare Earth Materials, Department of Chemistry, Tsinghua University, Beijing 100084, P. R. China*

Erbo Zhao − *Engineering Research Center of Advanced Rare Earth Materials, Department of Chemistry, Tsinghua University, Beijing 100084, P. R. China*

Yue Wu − *Engineering Research Center of Advanced Rare Earth Materials, Department of Chemistry, Tsinghua University, Beijing 100084, P. R. China*

Complete contact information is available at: https://pubs.acs.org/10.1021/jacsau.3c00001

Author Contributions

‡Jiazhan Li and Chang Chen contributed equally to this work. The manuscript was written through contributions of all authors. All authors have given approval to the final version of the manuscript.

Notes

The authors declare no competing financial interest.

■ ACKNOWLEDGMENTS

This work was supported by the National Key R&D Program of China (2021YFF0500503), the National Natural Science Foundation of China (21925202, U22B2071), the Beijing Municipal Natural Science Foundation (2214060), the China Postdoctoral Science Foundation (2020M680508), and the National Postdoctoral Program for Innovative Talents (BX20200180).

■ REFERENCES

(1) Liu, C.; Wu, Y.; Fang, J.; Yu, K.; Li, H.; He, W.; Cheong, W.-C.; Liu, S.; Chen, Z.; Dong, J.; Chen, C. Synergetic effect of nitrogen-doped carbon catalysts for high-efficiency electrochemical CO_2 reduction. *Chinese. J. Catal.* **2022**, *43* (7), 1697−1702.

(2) Luo, E.; Wang, C.; Li, Y.; Wang, X.; Gong, L.; Zhao, T.; Jin, Z.; Ge, J.; Liu, C.; Xing, W. Accelerated oxygen reduction on Fe/N/C catalysts derived from precisely-designed ZIF precursors. *Nano. Res.* **2020**, *13* (9), 2420−2426.

(3) Wu, K.; Sun, K.; Liu, S.; Cheong, W.-C.; Chen, Z.; Zhang, C.; Pan, Y.; Cheng, Y.; Zhuang, Z.; Wei, X.; Wang, Y.; Zheng, L.; Zhang, Q.; Wang, D.; Peng, Q.; Chen, C.; Li, Y. Atomically dispersed Ni−Ru−P interface sites for high-efficiency pH-universal electrocatalysis of hydrogen evolution. *Nano Energy* **2021**, *80*, 105467.

(4) Sun, K.; Zhao, L.; Zeng, L.; Liu, S.; Zhu, H.; Li, Y.; Chen, Z.; Zhuang, Z.; Li, Z.; Liu, Z.; Cao, D.; Zhao, J.; Liu, Y.; Pan, Y.; Chen, C. Reaction environment self-modification on low-coordination Ni^{2+} octahedra atomic interface for superior electrocatalytic overall water splitting. *Nano. Res.* **2020**, *13* (11), 3068−3074.

(5) Chen, C.; Kang, Y.; Huo, Z.; Zhu, Z.; Huang, W.; Xin, H. L.; Snyder, J. D.; Li, D.; Herron, J. A.; Mavrikakis, M.; Chi, M.; More, K. L.; Li, Y.; Markovic, N. M.; Somorjai, G. A.; Yang, P.; Stamenkovic, V. R. Highly crystalline multimetallic nanoframes with three-dimensional electrocatalytic surfaces. *Science* **2014**, *343* (6177), 1339−1343.

(6) Zhuang, Z.; Wang, Y.; Xu, C.-Q.; Liu, S.; Chen, C.; Peng, Q.; Zhuang, Z.; Xiao, H.; Pan, Y.; Lu, S.; Yu, R.; Cheong, W.-C.; Cao, X.; Wu, K.; Sun, K.; Wang, Y.; Wang, D.; Li, J.; Li, Y. Three-dimensional open nano-netcage electrocatalysts for efficient pH-universal overall water splitting. *Nat. Commun.* **2019**, *10* (1), 4875.

(7) Shah, K.; Dai, R.; Mateen, M.; Hassan, Z.; Zhuang, Z.; Liu, C.; Israr, M.; Cheong, W.-C.; Hu, B.; Tu, R.; Zhang, C.; Chen, X.; Peng, Q.; Chen, C.; Li, Y. Cobalt single atom incorporated in ruthenium oxide sphere: A robust bifunctional electrocatalyst for HER and OER. *Angew. Chem., Int. Ed.* **2022**, *61* (4), No. e202114951.

(8) Zhu, W.; Chen, C. Reaction: Open up the era of atomically precise catalysis. *Chem.* **2019**, *5* (11), 2737−2739.

(9) Hou, C.-C.; Zou, L.; Sun, L.; Zhang, K.; Liu, Z.; Li, Y.; Li, C.; Zou, R.; Yu, J.; Xu, Q. Single-atom iron catalysts on overhang-eave carbon cages for high-performance oxygen reduction reaction. *Angew. Chem., Int. Ed.* **2020**, *59* (19), 7384−7389.

(10) Hu, H.; Wang, J.; Cui, B.; Zheng, X.; Lin, J.; Deng, Y.; Han, X. Atomically dispersed selenium sites on nitrogen-doped carbon for efficient electrocatalytic oxygen reduction. *Angew. Chem., Int. Ed.* **2022**, *61* (3), No. e202114441.

(11) Tong, M.; Sun, F.; Xie, Y.; Wang, Y.; Yang, Y.; Tian, C.; Wang, L.; Fu, H. Operando cooperated catalytic mechanism of atomically dispersed $Cu-N_4$ and $Zn-N_4$ for promoting oxygen reduction reaction. *Angew. Chem., Int. Ed.* **2021**, *60* (25), 14005−14012.

(12) Li, F.; Han, G.-F.; Bu, Y.; Noh, H.-J.; Jeon, J.-P.; Shin, T. J.; Kim, S.-J.; Wu, Y.; Jeong, H. Y.; Fu, Z.; Lu, Y.; Baek, J.-B. Revealing isolated $M-N_3C_1$ active sites for efficient collaborative oxygen reduction catalysis. *Angew. Chem., Int. Ed.* **2020**, *59* (52), 23678−23683.

(13) Chen, S.; Luo, T.; Li, X.; Chen, K.; Fu, J.; Liu, K.; Cai, C.; Wang, Q.; Li, H.; Chen, Y.; Ma, C.; Zhu, L.; Lu, Y.-R.; Chan, T.-S.; Zhu, M.; Cortés, E.; Liu, M. Identification of the highly active $Co-N_4$ coordination motif for selective oxygen reduction to hydrogen peroxide. *J. Am. Chem. Soc.* **2022**, *144* (32), 14505−14516.

(14) Pan, Y.; Zhang, C.; Liu, Z.; Chen, C.; Li, Y. Structural regulation with atomic-level precision: From single-atomic site to diatomic and atomic interface catalysis. *Matter* **2020**, *2* (1), 78−110.

(15) Zhao, D.; Chen, Z.; Yang, W.; Liu, S.; Zhang, X.; Yu, Y.; Cheong, W.-C.; Zheng, L.; Ren, F.; Ying, G.; Cao, X.; Wang, D.; Peng, Q.; Wang, G.; Chen, C. MXene (Ti_3C_2) vacancy-confined single-atom catalyst for efficient functionalization of CO_2. *J. Am. Chem. Soc.* **2019**, *141* (9), 4086−4093.

(16) Zhu, Y.; Wang, J.; Koketsu, T.; Kroschel, M.; Chen, J.-M.; Hsu, S.-Y.; Henkelman, G.; Hu, Z.; Strasser, P.; Ma, J. Iridium single atoms incorporated in Co_3O_4 efficiently catalyze the oxygen evolution in acidic conditions. *Nat. Commun.* **2022**, *13* (1), 7754.

(17) Yan, J.; Kong, L.; Ji, Y.; White, J.; Li, Y.; Zhang, J.; An, P.; Liu, S.; Lee, S.-T.; Ma, T. Single atom tungsten doped ultrathin α-$Ni(OH)_2$ for enhanced electrocatalytic water oxidation. *Nat. Commun.* **2019**, *10* (1), 2149.

(18) Talib, S. H.; Lu, Z.; Yu, X.; Ahmad, K.; Bashir, B.; Yang, Z.; Li, J. Theoretical inspection of M1/PMA single-atom electrocatalyst: Ultra-high performance for water splitting (HER/OER) and oxygen reduction reactions (OER). *ACS Catal.* **2021**, *11* (14), 8929−8941.

(19) Shan, J.; Ye, C.; Jiang, Y.; Jaroniec, M.; Zheng, Y.; Qiao, S.-Z. Metal-metal interactions in correlated single-atom catalysts. *Sci. Adv.* **2022**, *8* (17), eabo0762.

(20) Lei, Z.; Cai, W.; Rao, Y.; Wang, K.; Jiang, Y.; Liu, Y.; Jin, X.; Li, J.; Lv, Z.; Jiao, S.; Zhang, W.; Yan, P.; Zhang, S.; Cao, R. Coordination modulation of iridium single-atom catalyst maximizing water oxidation activity. *Nat. Commun.* **2022**, *13* (1), 24.

(21) Bai, Y.; Yang, Z.; Feng, Y.; Liu, F.; Chen, X.; Chang, J. Preparation and electrocatalytic performance of Zn/N Co-doped carbon catalyst derived from MOF. *Chin. J. Inorg. Chem.* **2021**, *37* (6), 1055−1061.

(22) Kumar, A.; Zhang, Y.; Jia, Y.; Liu, W.; Sun, X. Redox chemistry of N_4-Fe^{2+} in iron phthalocyanines for oxygen reduction reaction. *Chinese. J. Catal.* **2021**, *42* (8), 1404−1412.

(23) Wu, K.; Chen, X.; Liu, S.; Pan, Y.; Cheong, W.-C.; Zhu, W.; Cao, X.; Shen, R.; Chen, W.; Luo, J.; Yan, W.; Zheng, L.; Chen, Z.; Wang, D.; Peng, Q.; Chen, C.; Li, Y. Porphyrin-like Fe-N_4 sites with sulfur adjustment on hierarchical porous carbon for different rate-determining steps in oxygen reduction reaction. *Nano. Res.* **2018**, *11* (12), 6260−6269.

(24) Yang, H.; Wang, X.; Zheng, T.; Cuello, N. C.; Goenaga, G.; Zawodzinski, T. A.; Tian, H.; Wright, J. T.; Meulenberg, R. W.; Wang, X.; Xia, Z.; Ma, S. CrN-encapsulated hollow Cr-N-C capsules boosting oxygen reduction catalysis in PEMFC. *CCS Chem.* **2021**, *3* (5), 208−218.
(25) Gu, Y.; Xi, B.; Tian, W.; Zhang, H.; Fu, Q.; Xiong, S. Boosting selective nitrogen reduction via geometric coordination engineering on single-tungsten-atom catalysts. *Adv. Mater.* **2021**, *33* (25), 2100429.
(26) Wang, Z.; Jin, X.; Zhu, C.; Liu, Y.; Tan, H.; Ku, R.; Zhang, Y.; Zhou, L.; Liu, Z.; Hwang, S.-J.; Fan, H. J. Atomically dispersed Co_2−N_6 and Fe−N_4 costructures boost oxygen reduction reaction in both alkaline and acidic media. *Adv. Mater.* **2021**, *33* (49), 2104718.
(27) Zhu, P.; Song, P.; Feng, W.; Zhao, D.; Liu, T.; Zhang, J.; Chen, C. Tailoring the selectivity and activity of oxygen reduction by regulating the coordination environments of carbon-supported atomically dispersed metal sites. *J. Mater. Chem. A* **2022**, *10* (35), 17948−17967.
(28) Zhao, D.; Yu, K.; Song, P.; Feng, W.; Hu, B.; Cheong, W.-C.; Zhuang, Z.; Liu, S.; Sun, K.; Zhang, J.; Chen, C. Atomic-level engineering $Fe_1N_2O_2$ interfacial structure derived from oxygen-abundant metal−organic frameworks to promote electrochemical CO_2 reduction. *Energy Environ. Sci.* **2022**, *15* (9), 3795−3804.
(29) Li, J.; Zhong, H.; Xu, M.; Li, T.; Wang, L.; Shi, Q.; Feng, S.; Lyu, Z.; Liu, D.; Du, D.; Beckman, S. P.; Pan, X.; Lin, Y.; Shao, M. Boosting the activity of Fe-N_x moieties in Fe-N-C electrocatalysts via phosphorus doping for oxygen reduction reaction. *Sci. China Mater.* **2020**, *63* (6), 965−971.
(30) Pan, Y.; Ma, X.; Wang, M.; Yang, X.; Liu, S.; Chen, H.-C.; Zhuang, Z.; Zhang, Y.; Cheong, W.-C.; Zhang, C.; Cao, X.; Shen, R.; Xu, Q.; Zhu, W.; Liu, Y.; Wang, X.; Zhang, X.; Yan, W.; Li, J.; Chen, H. M.; Chen, C.; Li, Y. Construction of N, P Co-doped carbon frames anchored with Fe single atoms and Fe_2P nanoparticles as a robust coupling catalyst for electrocatalytic oxygen reduction. *Adv. Mater.* **2022**, *34* (29), 2203621.
(31) Zhao, D.; Sun, K.; Cheong, W.-C.; Zheng, L.; Zhang, C.; Liu, S.; Cao, X.; Wu, K.; Pan, Y.; Zhuang, Z.; Hu, B.; Wang, D.; Peng, Q.; Chen, C.; Li, Y. Synergistically interactive pyridinic-N−MoP sites: identified active centers for enhanced hydrogen evolution in alkaline solution. *Angew. Chem., Int. Ed.* **2020**, *59* (23), 8982−8990.
(32) Pan, Y.; Sun, K.; Liu, S.; Cao, X.; Wu, K.; Cheong, W.-C.; Chen, Z.; Wang, Y.; Li, Y.; Liu, Y.; Wang, D.; Peng, Q.; Chen, C.; Li, Y. Core−shell ZIF-8@ZIF-67-derived CoP nanoparticle-embedded N-doped carbon nanotube hollow polyhedron for efficient overall water splitting. *J. Am. Chem. Soc.* **2018**, *140* (7), 2610−2618.
(33) Du, L.; Prabhakaran, V.; Xie, X.; Park, S.; Wang, Y.; Shao, Y. Low-PGM and PGM-free catalysts for proton exchange membrane fuel cells: stability challenges and material solutions. *Adv. Mater.* **2021**, *33* (6), 1908232.
(34) Liu, J.; Wan, X.; Liu, S.; Liu, X.; Zheng, L.; Yu, R.; Shui, J. Hydrogen passivation of M−N−C (M = Fe, Co) catalysts for storage stability and ORR activity improvements. *Adv. Mater.* **2021**, *33* (38), 2103600.
(35) Shao, Y.; Dodelet, J.-P.; Wu, G.; Zelenay, P. PGM-free cathode catalysts for PEM fuel cells: a mini-review on stability challenges. *Adv. Mater.* **2019**, *31* (31), 1807615.
(36) Martinez, U.; Komini Babu, S.; Holby, E. F.; Chung, H. T.; Yin, X.; Zelenay, P. Progress in the development of Fe-based PGM-free electrocatalysts for the oxygen reduction reaction. *Adv. Mater.* **2019**, *31* (31), 1806545.
(37) Qiao, B.; Wang, A.; Yang, X.; Allard, L. F.; Jiang, Z.; Cui, Y.; Liu, J.; Li, J.; Zhang, T. Single-atom catalysis of CO oxidation using Pt_1/FeO_x. *Nat. Chem.* **2011**, *3* (8), 634−641.
(38) Su, P.; Huang, W.; Zhang, J.; Guharoy, U.; Du, Q.; Sun, Q.; Jiang, Q.; Cheng, Y.; Yang, J.; Zhang, X.; Liu, Y.; Jiang, S. P.; Liu, J. Fe atoms anchored on defective nitrogen doped hollow carbon spheres as efficient electrocatalysts for oxygen reduction reaction. *Nano. Res.* **2021**, *14* (4), 1069−1077.
(39) Ding, L.; Tang, T.; Hu, J.-S. Recent progress in proton-exchange membrane fuel cells based on metal-nitrogen-carbon catalysts. *Acta Phys.-Chim. Sin.* **2020**, *37* (9), 2010048.
(40) Zhang, H.; Hwang, S.; Wang, M.; Feng, Z.; Karakalos, S.; Luo, L.; Qiao, Z.; Xie, X.; Wang, C.; Su, D.; Shao, Y.; Wu, G. Single atomic iron catalysts for oxygen reduction in acidic media: particle size control and thermal activation. *J. Am. Chem. Soc.* **2017**, *139* (40), 14143−14149.
(41) Xiong, W.; Li, H.; Wang, H.; Yi, J.; You, H.; Zhang, S.; Hou, Y.; Cao, M.; Zhang, T.; Cao, R. Hollow mesoporous carbon sphere loaded Ni−N_4 single-atom: support structure study for CO_2 electrocatalytic reduction catalyst. *Small* **2020**, *16* (41), 2003943.
(42) Chen, Y.; Ji, S.; Wang, Y.; Dong, J.; Chen, W.; Li, Z.; Shen, R.; Zheng, L.; Zhuang, Z.; Wang, D.; Li, Y. Isolated single iron atoms anchored on N-doped porous carbon as an efficient electrocatalyst for the oxygen reduction reaction. *Angew. Chem., Int. Ed.* **2017**, *56* (24), 6937−6941.
(43) Tang, L.; Yu, L.; Ma, C.; Song, Y.; Tu, Y.; Zhang, Y.; Bo, X.; Deng, D. Three-dimensional CoOOH nanoframes confining high-density Mo single atoms for large-current-density oxygen evolution. *J. Mater. Chem. A* **2022**, *10* (11), 6242−6250.
(44) Wang, Q.; Huang, X.; Zhao, Z. L.; Wang, M.; Xiang, B.; Li, J.; Feng, Z.; Xu, H.; Gu, M. Ultrahigh-loading of Ir single atoms on NiO matrix to dramatically enhance oxygen evolution reaction. *J. Am. Chem. Soc.* **2020**, *142* (16), 7425−7433.
(45) Li, J.; Jiang, Y.-f.; Wang, Q.; Xu, C.-Q.; Wu, D.; Banis, M. N.; Adair, K. R.; Doyle-Davis, K.; Meira, D. M.; Finfrock, Y. Z.; Li, W.; Zhang, L.; Sham, T.-K.; Li, R.; Chen, N.; Gu, M.; Li, J.; Sun, X. A general strategy for preparing pyrrolic-N_4 type single-atom catalysts via pre-located isolated atoms. *Nat. Commun.* **2021**, *12* (1), 6806.
(46) Cao, D.; Zhang, Z.; Cui, Y.; Zhang, R.; Zhang, L.; Zeng, J.; Cheng, D. One-step approach for constructing high density single-atom catalysts toward overall water splitting at industrial current densities. *Angew. Chem., Int. Ed.* **2023**, No. e202214259.
(47) Li, J.; Chen, M.; Cullen, D. A.; Hwang, S.; Wang, M.; Li, B.; Liu, K.; Karakalos, S.; Lucero, M.; Zhang, H.; Lei, C.; Xu, H.; Sterbinsky, G. E.; Feng, Z.; Su, D.; More, K. L.; Wang, G.; Wang, Z.; Wu, G. Atomically dispersed manganese catalysts for oxygen reduction in proton-exchange membrane fuel cells. *Nat. Catal.* **2018**, *1* (12), 935−945.
(48) Liu, S.; Li, C.; Zachman, M. J.; Zeng, Y.; Yu, H.; Li, B.; Wang, M.; Braaten, J.; Liu, J.; Meyer, H. M.; Lucero, M.; Kropf, A. J.; Alp, E. E.; Gong, Q.; Shi, Q.; Feng, Z.; Xu, H.; Wang, G.; Myers, D. J.; Xie, J.; Cullen, D. A.; Litster, S.; Wu, G. Atomically dispersed iron sites with a nitrogen−carbon coating as highly active and durable oxygen reduction catalysts for fuel cells. *Nat. Energy* **2022**, *7* (7), 652−663.
(49) Qu, Y.; Li, Z.; Chen, W.; Lin, Y.; Yuan, T.; Yang, Z.; Zhao, C.; Wang, J.; Zhao, C.; Wang, X.; Zhou, F.; Zhuang, Z.; Wu, Y.; Li, Y. Direct transformation of bulk copper into copper single sites via emitting and trapping of atoms. *Nat. Catal.* **2018**, *1* (10), 781−786.
(50) Wei, S.; Li, A.; Liu, J.-C.; Li, Z.; Chen, W.; Gong, Y.; Zhang, Q.; Cheong, W.-C.; Wang, Y.; Zheng, L.; Xiao, H.; Chen, C.; Wang, D.; Peng, Q.; Gu, L.; Han, X.; Li, J.; Li, Y. Direct observation of noble metal nanoparticles transforming to thermally stable single atoms. *Nat. Nanotechnol.* **2018**, *13* (9), 856−861.
(51) Li, J.; Zhang, H.; Samarakoon, W.; Shan, W.; Cullen, D. A.; Karakalos, S.; Chen, M.; Gu, D.; More, K. L.; Wang, G.; Feng, Z.; Wang, Z.; Wu, G. Thermally driven structure and performance evolution of atomically dispersed FeN_4 sites for oxygen reduction. *Angew. Chem., Int. Ed.* **2019**, *58* (52), 18971−18980.
(52) Chen, R.; Yang, C.; Cai, W.; Wang, H.-Y.; Miao, J.; Zhang, L.; Chen, S.; Liu, B. Use of platinum as the counter electrode to study the activity of nonprecious metal catalysts for the hydrogen evolution reaction. *ACS Energy Lett.* **2017**, *2* (5), 1070−1075.
(53) Zhang, L.; Han, L.; Liu, H.; Liu, X.; Luo, J. Potential-cycling synthesis of single platinum atoms for efficient hydrogen evolution in neutral media. *Angew. Chem., Int. Ed.* **2017**, *56* (44), 13694−13698.
(54) Wan, X.; Liu, X.; Li, Y.; Yu, R.; Zheng, L.; Yan, W.; Wang, H.; Xu, M.; Shui, J. Fe−N−C electrocatalyst with dense active sites and

https://doi.org/10.1021/jacsau.3c00001
JACS Au 2023, 3, 736−755

efficient mass transport for high-performance proton exchange membrane fuel cells. *Nat. Catal.* **2019**, *2* (3), 259−268.
(55) Jiao, L.; Li, J.; Richard, L. L.; Sun, Q.; Stracensky, T.; Liu, E.; Sougrati, M. T.; Zhao, Z.; Yang, F.; Zhong, S.; Xu, H.; Mukerjee, S.; Huang, Y.; Cullen, D. A.; Park, J. H.; Ferrandon, M.; Myers, D. J.; Jaouen, F.; Jia, Q. Chemical vapour deposition of Fe−N−C oxygen reduction catalysts with full utilization of dense Fe−N_4 sites. *Nat. Mater.* **2021**, *20* (10), 1385−1391.
(56) Zhao, Y.; Lu, X. F.; Fan, G.; Luan, D.; Gu, X.; Lou, X. W. Surface-exposed single-Ni atoms with potential-driven dynamic behaviors for highly efficient electrocatalytic oxygen evolution. *Angew. Chem., Int. Ed.* **2022**, *61* (45), No. e202212542.
(57) Pan, Y.; Liu, S.; Sun, K.; Chen, X.; Wang, B.; Wu, K.; Cao, X.; Cheong, W.-C.; Shen, R.; Han, A.; Chen, Z.; Zheng, L.; Luo, J.; Lin, Y.; Liu, Y.; Wang, D.; Peng, Q.; Zhang, Q.; Chen, C.; Li, Y. A bimetallic Zn/Fe Polyphthalocyanine-derived single-atom Fe-N_4 catalytic site: a superior trifunctional catalyst for overall water splitting and Zn−air batteries. *Angew. Chem., Int. Ed.* **2018**, *57* (28), 8614−8618.
(58) Jin, Z.; Li, P.; Meng, Y.; Fang, Z.; Xiao, D.; Yu, G. Understanding the inter-site distance effect in single-atom catalysts for oxygen electroreduction. *Nat. Catal.* **2021**, *4* (7), 615−622.
(59) Li, J.; Sougrati, M. T.; Zitolo, A.; Ablett, J. M.; Oğuz, I. C.; Mineva, T.; Matanovic, I.; Atanassov, P.; Huang, Y.; Zenyuk, I.; Di Cicco, A.; Kumar, K.; Dubau, L.; Maillard, F.; Dražić, G.; Jaouen, F. Identification of durable and non-durable FeN_x sites in Fe−N−C materials for proton exchange membrane fuel cells. *Nat. Catal.* **2021**, *4* (1), 10−19.
(60) Cao, D.; Xu, H.; Li, H.; Feng, C.; Zeng, J.; Cheng, D. Volcano-type relationship between oxidation states and catalytic activity of single-atom catalysts towards hydrogen evolution. *Nat. Commun.* **2022**, *13* (1), 5843.
(61) Yuan, K.; Lützenkirchen-Hecht, D.; Li, L.; Shuai, L.; Li, Y.; Cao, R.; Qiu, M.; Zhuang, X.; Leung, M. K. H.; Chen, Y.; Scherf, U. Boosting oxygen reduction of single iron active sites via geometric and electronic engineering: nitrogen and phosphorus dual coordination. *J. Am. Chem. Soc.* **2020**, *142* (5), 2404−2412.
(62) Zhao, Y.; Zhang, Z.; Liu, L.; Wang, Y.; Wu, T.; Qin, W.; Liu, S.; Jia, B.; Wu, H.; Zhang, D.; Qu, X.; Qi, G.; Giannelis, E. P.; Qin, M.; Guo, S. S and O Co-coordinated Mo single sites in hierarchically porous tubes from sulfur−enamine copolymerization for oxygen reduction and evolution. *J. Am. Chem. Soc.* **2022**, *144* (45), 20571−20581.
(63) Tang, C.; Chen, L.; Li, H.; Li, L.; Jiao, Y.; Zheng, Y.; Xu, H.; Davey, K.; Qiao, S.-Z. Tailoring acidic oxygen reduction selectivity on single-atom catalysts via modification of first and second coordination spheres. *J. Am. Chem. Soc.* **2021**, *143* (20), 7819−7827.
(64) Zhang, J.; Chen, G.; Liu, Q.; Fan, C.; Sun, D.; Tang, Y.; Sun, H.; Feng, X. Competitive adsorption: Reducing the poisoning effect of adsorbed hydroxyl on Ru single-atom site with SnO_2 for efficient hydrogen evolution. *Angew. Chem., Int. Ed.* **2022**, *61* (39), No. e202209486.
(65) Wang, D.; Xue, J.; Ding, X.; Wei, J.; Feng, C.; Wang, R.; Ma, P.; Wang, S.; Cao, H.; Wang, J.; Zuo, M.; Zhou, S.; Zhang, Z.; Zeng, J.; Bao, J. Neighboring cationic vacancy assisted adsorption optimization on single-atom sites for improved oxygen eolution. *ACS Catal.* **2022**, *12* (19), 12458−12468.
(66) Chen, K.; Liu, K.; An, P.; Li, H.; Lin, Y.; Hu, J.; Jia, C.; Fu, J.; Li, H.; Liu, H.; Lin, Z.; Li, W.; Li, J.; Lu, Y.-R.; Chan, T.-S.; Zhang, N.; Liu, M. Iron phthalocyanine with coordination induced electronic localization to boost oxygen reduction reaction. *Nat. Commun.* **2020**, *11* (1), 4173.
(67) Wu, Y.; Chen, C.; Yan, X.; Sun, X.; Zhu, Q.; Li, P.; Li, Y.; Liu, S.; Ma, J.; Huang, Y.; Han, B. Boosting CO_2 electroreduction over a cadmium single-atom catalyst by tuning of the axial coordination structure. *Angew. Chem., Int. Ed.* **2021**, *60* (38), 20803−20810.
(68) Cao, L.; Luo, Q.; Liu, W.; Lin, Y.; Liu, X.; Cao, Y.; Zhang, W.; Wu, Y.; Yang, J.; Yao, T.; Wei, S. Identification of single-atom active sites in carbon-based cobalt catalysts during electrocatalytic hydrogen evolution. *Nat. Catal.* **2019**, *2* (2), 134−141.
(69) Chen, Z.; Huang, A.; Yu, K.; Cui, T.; Zhuang, Z.; Liu, S.; Li, J.; Tu, R.; Sun, K.; Tan, X.; Zhang, J.; Liu, D.; Zhang, Y.; Jiang, P.; Pan, Y.; Chen, C.; Peng, Q.; Li, Y. Fe_1N_4−O_1 site with axial Fe−O coordination for highly selective CO_2 reduction over a wide potential range. *Energy Environ. Sci.* **2021**, *14* (6), 3430−3437.
(70) Chen, C.; Chen, Z.; Zhong, J.; Song, X.; Chen, D.; Liu, S.; Cheong, W.-C.; Li, J.; Tan, X.; He, C.; Zhang, J.; Liu, D.; Yuan, Q.; Chen, C.; Peng, Q.; Li, Y., Regulating electronic structure of CoN_4 with axial Co-S for promoting oxygen reduction and Zn-air battery performance. *Nano. Res.* **2022**. DOI: 10.1007/s12274-022-5164-y
(71) Huang, Z.; Tang, Q. Axial coordination effect on the oxygen reduction reaction of FeN_4 electrocatalysts based on grand canonical density functional theory. *J. Phys. Chem. C* **2022**, *126* (51), 21606−21615.
(72) Zhang, T.; Jin, J.; Chen, J.; Fang, Y.; Han, X.; Chen, J.; Li, Y.; Wang, Y.; Liu, J.; Wang, L. Pinpointing the axial ligand effect on platinum single-atom-catalyst towards efficient alkaline hydrogen evolution reaction. *Nat. Commun.* **2022**, *13* (1), 6875.
(73) Jiao, J.; Lin, R.; Liu, S.; Cheong, W.-C.; Zhang, C.; Chen, Z.; Pan, Y.; Tang, J.; Wu, K.; Hung, S.-F.; Chen, H. M.; Zheng, L.; Lu, Q.; Yang, X.; Xu, B.; Xiao, H.; Li, J.; Wang, D.; Peng, Q.; Chen, C.; Li, Y. Copper atom-pair catalyst anchored on alloy nanowires for selective and efficient electrochemical reduction of CO_2. *Nat. Chem.* **2019**, *11* (3), 222−228.
(74) Li, Y.; Chen, C.; Cao, R.; Pan, Z.; He, H.; Zhou, K. Dual-atom Ag_2/graphene catalyst for efficient electroreduction of CO_2 to CO. *Appl. Catal., B* **2020**, *268*, 118747.
(75) Kumar, A.; Bui, V. Q.; Lee, J.; Wang, L.; Jadhav, A. R.; Liu, X.; Shao, X.; Liu, Y.; Yu, J.; Hwang, Y.; Bui, H. T. D.; Ajmal, S.; Kim, M. G.; Kim, S.-G.; Park, G.-S.; Kawazoe, Y.; Lee, H. Moving beyond bimetallic-alloy to single-atom dimer atomic-interface for all-pH hydrogen evolution. *Nat. Commun.* **2021**, *12* (1), 6766.
(76) Bai, L.; Hsu, C.-S.; Alexander, D. T. L.; Chen, H. M.; Hu, X. A cobalt−iron double-atom catalyst for the oxygen evolution reaction. *J. Am. Chem. Soc.* **2019**, *141* (36), 14190−14199.
(77) Zhu, P.; Xiong, X.; Wang, X.; Ye, C.; Li, J.; Sun, W.; Sun, X.; Jiang, J.; Zhuang, Z.; Wang, D.; Li, Y. Regulating the FeN_4 moiety by constructing Fe−Mo dual-metal atom sites for efficient electrochemical oxygen reduction. *Nano Lett.* **2022**, *22* (23), 9507−9515.
(78) Yang, Y.; Qian, Y.; Li, H.; Zhang, Z.; Mu, Y.; Do, D.; Zhou, B.; Dong, J.; Yan, W.; Qin, Y.; Fang, L.; Feng, R.; Zhou, J.; Zhang, P.; Dong, J.; Yu, G.; Liu, Y.; Zhang, X.; Fan, X. O-coordinated W-Mo dual-atom catalyst for pH-universal electrocatalytic hydrogen evolution. *Sci. Adv.* **2020**, *6* (23), eaba6586.
(79) Yin, Z.; Yu, J.; Xie, Z.; Yu, S.-W.; Zhang, L.; Akauola, T.; Chen, J. G.; Huang, W.; Qi, L.; Zhang, S. Hybrid catalyst coupling single-atom Ni and nanoscale Cu for efficient CO_2 electroreduction to ethylene. *J. Am. Chem. Soc.* **2022**, *144* (45), 20931−20938.
(80) Su, P.; Pei, W.; Wang, X.; Ma, Y.; Jiang, Q.; Liang, J.; Zhou, S.; Zhao, J.; Liu, J.; Lu, G. Q. Exceptional electrochemical HER performance with enhanced electron transfer between Ru nanoparticles and single atoms dispersed on a carbon substrate. *Angew. Chem., Int. Ed.* **2021**, *60* (29), 16044−16050.
(81) Xiao, F.; Wang, Q.; Xu, G.-L.; Qin, X.; Hwang, I.; Sun, C.-J.; Liu, M.; Hua, W.; Wu, H.-w.; Zhu, S.; Li, J.-C.; Wang, J.-G.; Zhu, Y.; Wu, D.; Wei, Z.; Gu, M.; Amine, K.; Shao, M. Atomically dispersed Pt and Fe sites and Pt−Fe nanoparticles for durable proton exchange membrane fuel cells. *Nat. Catal.* **2022**, *5* (6), 503−512.
(82) Zhang, T.; Zheng, P.; Gu, F.; Xu, W.; Chen, W.; Zhu, T.; Han, Y.-F.; Xu, G.; Zhong, Z.; Su, F. The dual-active-site tandem catalyst containing Ru single atoms and Ni nanoparticles boosts CO_2 methanation. *Appl. Catal., B* **2023**, *323*, 122190.
(83) Chen, H.; Chen, S.; Zhang, Z.; Sheng, L.; Zhao, J.; Fu, W.; Xi, S.; Si, R.; Wang, L.; Fan, M.; Yang, B. Single-atom-induced adsorption optimization of adjacent sites boosted oxygen evolution reaction. *ACS Catal.* **2022**, *12* (21), 13482−13491.

(84) Huo, L.; Jin, C.; Tang, J.; Xu, X.; Jiang, K.; Shang, L.; Li, Y.; Zhang, J.; Zhu, L.; Chu, J.; Hu, Z. Ultrathin NiPt single-atom alloy for synergistically accelerating alkaline hydrogen evolution. *ACS Appl. Energy Mater.* **2022**, *5* (12), 15136−15145.
(85) Jiang, K.; Siahrostami, S.; Zheng, T.; Hu, Y.; Hwang, S.; Stavitski, E.; Peng, Y.; Dynes, J.; Gangisetty, M.; Su, D.; Attenkofer, K.; Wang, H. Isolated Ni single atoms in graphene nanosheets for high-performance CO_2 reduction. *Energy Environ. Sci.* **2018**, *11* (4), 893−903.
(86) Jiang, H.; Yang, W.; Xu, M.; Wang, E.; Wei, Y.; Liu, W.; Gu, X.; Liu, L.; Chen, Q.; Zhai, P.; Zou, X.; Ajayan, P. M.; Zhou, W.; Gong, Y. Single atom catalysts in Van der Waals gaps. *Nat. Commun.* **2022**, *13* (1), 6863.
(87) Song, H.; Wu, M.; Tang, Z.; Tse, J. S.; Yang, B.; Lu, S. Single atom ruthenium-doped CoP/CDs nanosheets via splicing of carbon-dots for robust hydrogen production. *Angew. Chem., Int. Ed.* **2021**, *60* (13), 7234−7244.
(88) Liu, C.; Wu, Y.; Sun, K.; Fang, J.; Huang, A.; Pan, Y.; Cheong, W.-C.; Zhuang, Z.; Zhuang, Z.; Yuan, Q.; Xin, H. L.; Zhang, C.; Zhang, J.; Xiao, H.; Chen, C.; Li, Y. Constructing FeN_4/graphitic nitrogen atomic interface for high-efficiency electrochemical CO_2 reduction over a broad potential window. *Chem.* **2021**, *7* (5), 1297−1307.
(89) Qiao, Z.; Hwang, S.; Li, X.; Wang, C.; Samarakoon, W.; Karakalos, S.; Li, D.; Chen, M.; He, Y.; Wang, M.; Liu, Z.; Wang, G.; Zhou, H.; Feng, Z.; Su, D.; Spendelow, J. S.; Wu, G. 3D porous graphitic nanocarbon for enhancing the performance and durability of Pt catalysts: a balance between graphitization and hierarchical porosity. *Energy Environ. Sci.* **2019**, *12* (9), 2830−2841.
(90) Xie, X.; He, C.; Li, B.; He, Y.; Cullen, D. A.; Wegener, E. C.; Kropf, A. J.; Martinez, U.; Cheng, Y.; Engelhard, M. H.; Bowden, M. E.; Song, M.; Lemmon, T.; Li, X. S.; Nie, Z.; Liu, J.; Myers, D. J.; Zelenay, P.; Wang, G.; Wu, G.; Ramani, V.; Shao, Y. Performance enhancement and degradation mechanism identification of a single-atom Co−N−C catalyst for proton exchange membrane fuel cells. *Nat. Catal.* **2020**, *3* (12), 1044−1054.
(91) Pan, Y.; Lin, R.; Chen, Y.; Liu, S.; Zhu, W.; Cao, X.; Chen, W.; Wu, K.; Cheong, W.-C.; Wang, Y.; Zheng, L.; Luo, J.; Lin, Y.; Liu, Y.; Liu, C.; Li, J.; Lu, Q.; Chen, X.; Wang, D.; Peng, Q.; Chen, C.; Li, Y. Design of single-atom Co−N_5 catalytic site: A robust electrocatalyst for CO_2 reduction with nearly 100% CO selectivity and remarkable stability. *J. Am. Chem. Soc.* **2018**, *140* (12), 4218−4221.
(92) Cheng, N.; Stambula, S.; Wang, D.; Banis, M. N.; Liu, J.; Riese, A.; Xiao, B.; Li, R.; Sham, T.-K.; Liu, L.-M.; Botton, G. A.; Sun, X. Platinum single-atom and cluster catalysis of the hydrogen evolution reaction. *Nat. Commun.* **2016**, *7* (1), 13638.
(93) Liu, Y.; Liu, X.; Jadhav, A. R.; Yang, T.; Hwang, Y.; Wang, H.; Wang, L.; Luo, Y.; Kumar, A.; Lee, J.; Bui, H. T. D.; Gyu Kim, M.; Lee, H. Unraveling the function of metal−amorphous support interactions in single-atom electrocatalytic hydrogen evolution. *Angew. Chem., Int. Ed.* **2022**, *61* (9), No. e202114160.
(94) Jiang, R.; Li, L.; Sheng, T.; Hu, G.; Chen, Y.; Wang, L. Edge-site engineering of atomically dispersed Fe−N_4 by selective C−N bond cleavage for enhanced oxygen reduction reaction activities. *J. Am. Chem. Soc.* **2018**, *140* (37), 11594−11598.
(95) Wang, Q.; Zhang, Z.; Cai, C.; Wang, M.; Zhao, Z. L.; Li, M.; Huang, X.; Han, S.; Zhou, H.; Feng, Z.; Li, L.; Li, J.; Xu, H.; Francisco, J. S.; Gu, M. Single iridium atom doped Ni_2P catalyst for optimal oxygen evolution. *J. Am. Chem. Soc.* **2021**, *143* (34), 13605−13615.
(96) Wang, Y.; Chen, Z.; Han, P.; Du, Y.; Gu, Z.; Xu, X.; Zheng, G. Single-atomic Cu with multiple oxygen vacancies on ceria for electrocatalytic CO_2 reduction to CH_4. *ACS Catal.* **2018**, *8* (8), 7113−7119.
(97) Wang, F.; Zhou, Y.; Lin, S.; Yang, L.; Hu, Z.; Xie, D. Axial ligand effect on the stability of Fe−N−C electrocatalysts for acidic oxygen reduction reaction. *Nano Energy* **2020**, *78*, 105128.
(98) Bai, X.; Zhao, X.; Zhang, Y.; Ling, C.; Zhou, Y.; Wang, J.; Liu, Y. Dynamic stability of copper single-atom catalysts under working conditions. *J. Am. Chem. Soc.* **2022**, *144* (37), 17140−17148.
(99) Rivera-Cárcamo, C.; Serp, P. Single atom catalysts on carbon-based materials. *ChemCatChem.* **2018**, *10* (22), 5058−5091.
(100) He, F.; Li, K.; Yin, C.; Wang, Y.; Tang, H.; Wu, Z. Single Pd atoms supported by graphitic carbon nitride, a potential oxygen reduction reaction catalyst from theoretical perspective. *Carbon* **2017**, *114*, 619−627.
(101) Wang, X.; Fu, N.; Liu, J.-C.; Yu, K.; Li, Z.; Xu, Z.; Liang, X.; Zhu, P.; Ye, C.; Zhou, A.; Li, A.; Zheng, L.; Liu, L.-M.; Chen, C.; Wang, D.; Peng, Q.; Li, Y. Atomic replacement of PtNi nanoalloys within Zn-ZIF-8 for the fabrication of a multisite CO_2 reduction electrocatalyst. *J. Am. Chem. Soc.* **2022**, *144* (50), 23223−23229.
(102) Kuznetsov, D. A.; Chen, Z.; Abdala, P. M.; Safonova, O. V.; Fedorov, A.; Müller, C. R. Single-atom-substituted Mo_2CT_x:Fe-layered carbide for selective oxygen reduction to hydrogen peroxide: tracking the evolution of the MXene phase. *J. Am. Chem. Soc.* **2021**, *143* (15), 5771−5778.
(103) Yang, J.; Liu, W.; Xu, M.; Liu, X.; Qi, H.; Zhang, L.; Yang, X.; Niu, S.; Zhou, D.; Liu, Y.; Su, Y.; Li, J.-F.; Tian, Z.-Q.; Zhou, W.; Wang, A.; Zhang, T. Dynamic behavior of single-atom catalysts in electrocatalysis: Identification of Cu-N_3 as an active site for the oxygen reduction reaction. *J. Am. Chem. Soc.* **2021**, *143* (36), 14530−14539.
(104) Zhang, Y.; Jiao, L.; Yang, W.; Xie, C.; Jiang, H.-L. Rational fabrication of low-coordinate single-atom Ni electrocatalysts by MOFs for highly selective CO_2 reduction. *Angew. Chem., Int. Ed.* **2021**, *60* (14), 7607−7611.
(105) Matsubu, J. C.; Yang, V. N.; Christopher, P. Isolated metal active site concentration and stability control catalytic CO_2 reduction selectivity. *J. Am. Chem. Soc.* **2015**, *137* (8), 3076−3084.
(106) Guo, W.; Tan, X.; Bi, J.; Xu, L.; Yang, D.; Chen, C.; Zhu, Q.; Ma, J.; Tayal, A.; Ma, J.; Huang, Y.; Sun, X.; Liu, S.; Han, B. Atomic indium catalysts for switching CO_2 electroreduction products from formate to CO. *J. Am. Chem. Soc.* **2021**, *143* (18), 6877−6885.
(107) Sun, K.; Yu, K.; Fang, J.; Zhuang, Z.; Tan, X.; Wu, Y.; Zeng, L.; Zhuang, Z.; Pan, Y.; Chen, C. Nature-inspired design of molybdenum−selenium dual-single-atom electrocatalysts for CO_2 reduction. *Adv. Mater.* **2022**, *34* (44), 2206478.
(108) Duan, H.; Wang, C.; Li, G.; Tan, H.; Hu, W.; Cai, L.; Liu, W.; Li, N.; Ji, Q.; Wang, Y.; Lu, Y.; Yan, W.; Hu, F.; Zhang, W.; Sun, Z.; Qi, Z.; Song, L.; Wei, S. Single-atom-layer catalysis in a MoS_2 monolayer activated by long-range ferromagnetism for the hydrogen evolution reaction: beyond single-atom catalysis. *Angew. Chem., Int. Ed.* **2021**, *60* (13), 7251−7258.
(109) Li, J.; Jiao, L.; Wegener, E.; Richard, L. L.; Liu, E.; Zitolo, A.; Sougrati, M. T.; Mukerjee, S.; Zhao, Z.; Huang, Y.; Yang, F.; Zhong, S.; Xu, H.; Kropf, A. J.; Jaouen, F.; Myers, D. J.; Jia, Q. Evolution pathway from iron compounds to Fe_1(II)−N_4 sites through gas-phase iron during pyrolysis. *J. Am. Chem. Soc.* **2020**, *142* (3), 1417−1423.
(110) Zhang, E.; Wang, T.; Yu, K.; Liu, J.; Chen, W.; Li, A.; Rong, H.; Lin, R.; Ji, S.; Zheng, X.; Wang, Y.; Zheng, L.; Chen, C.; Wang, D.; Zhang, J.; Li, Y. Bismuth single atoms resulting from transformation of metal−organic frameworks and their use as electrocatalysts for CO_2 reduction. *J. Am. Chem. Soc.* **2019**, *141* (42), 16569−16573.
(111) Suwanpinij, P.; Worabut, A.; Supruangnet, R.; Henning Dickert, H. Analysis of precipitation and dissolution of the microalloying elements by X-ray absorption spectroscopy (XAS). *AIMS Mater. Sci.* **2017**, *4* (4), 856−866.
(112) He, Q.; Lee, J. H.; Liu, D.; Liu, Y.; Lin, Z.; Xie, Z.; Hwang, S.; Kattel, S.; Song, L.; Chen, J. G. Accelerating CO_2 electroreduction to CO over Pd single-atom catalyst. *Adv. Funct. Mater.* **2020**, *30* (17), 2000407.
(113) Gu, J.; Hsu, C.-S.; Bai, L.; Chen, H. M.; Hu, X. Atomically dispersed Fe^{3+} sites catalyze efficient CO_2 electroreduction to CO. *Science* **2019**, *364* (6445), 1091−1094.

https://doi.org/10.1021/jacsau.3c00001
JACS Au 2023, 3, 736−755

(114) Xiao, M.; Gao, L.; Wang, Y.; Wang, X.; Zhu, J.; Jin, Z.; Liu, C.; Chen, H.; Li, G.; Ge, J.; He, Q.; Wu, Z.; Chen, Z.; Xing, W. Engineering energy level of metal center: Ru single-atom site for efficient and durable oxygen reduction catalysis. *J. Am. Chem. Soc.* **2019**, *141* (50), 19800−19806.
(115) Li, X.; Cao, C.-S.; Hung, S.-F.; Lu, Y.-R.; Cai, W.; Rykov, A. I.; Miao, S.; Xi, S.; Yang, H.; Hu, Z.; Wang, J.; Zhao, J.; Alp, E. E.; Xu, W.; Chan, T.-S.; Chen, H.; Xiong, Q.; Xiao, H.; Huang, Y.; Li, J.; Zhang, T.; Liu, B. Identification of the electronic and structural dynamics of catalytic centers in single-Fe-atom material. *Chem.* **2020**, *6* (12), 3440−3454.

https://doi.org/10.1021/jacsau.3c00001
JACS Au 2023, 3, 736−755